2

DOE/MC/22065--2809

DE90 000441

Low-Temperature, Sulfur-Tolerant Homogeneous Catalysts for the Water-Gas Shift Reaction

Final Report

R.B. Wilson, Jr.
M.F. Asaro
E.J. Crawford
B.J. Wood
R.M. Laine
R.H. Schwaar

December 1989

Work Performed Under Contract No.: DE-AC21-85MC22065

For
U.S. Department of Energy
Office of Fossil Energy
Morgantown Energy Technology Center
Morgantown, West Virginia

By
SRI International
Menlo Park, California

DISCLAIMER

Available to DOE and DOE contractors from the Office of Scientific and Technical Information, P.O. Box 62, Oak Ridge, TN 37831; prices available from (615)576-8401, FTS 626-8401.

Available to the public from the National Technical Information Service, U.S. Department of Commerce, 5285 Port Royal Rd., Springfield, VA 22161.

Price: Printed copy AO6
Microfiche AO1

Codes are used for pricing all publications. The code is determined by the number of pages in the publication. Information pertaining to the pricing codes can be found in the current issues of the following publications, which are generally available in most libraries: *Energy Research Abstracts (ERA), Government Reports Announcements* and *Index (GRA* and *I); Scientific and Technical Abstracts Reports (STAR);* and publication NTIS-PR-360 available from NTIS at the above address.

DOE/MC/22065-2809
(DE90000441)

Low-Temperature, Sulfur-Tolerant Homogeneous Catalysts for the Water-Gas Shift Reaction

Final Report

R.B. Wilson, Jr.
M.F. Asaro
E.J. Crawford
B.J. Wood
R.M. Laine
R.H. Schwaar

Work Performed Under Contract No.: DE-AC21-85MC22065

For
U.S. Department of Energy
Office of Fossil Energy
Morgantown Energy Technology Center
P.O. Box 880
Morgantown, West Virginia 26507-0880

By
SRI International
333 Ravenswood Avenue
Menlo Park, California 94025-3493

December 1989

ABSTRACT

Coal gasification in conjunction with the water-gas shift reaction represents a significant resource for the production of hydrogen, a gas of considerable industrial value. Current industrial water-gas shift reaction (WGSR) processes are operated in two stages: a high temperature shift (HTS) stage operating at about 350°C over sulfur-tolerant catalysts, followed by a low temperature shift (LTS) stage operating at about 250°C over a sulfur-intolerant catalyst. The HTS is required because sulfur is present in the feed gas and for the high conversion rates obtainable over such catalysts at high temperature. The LTS is required because of the inverse temperature dependence of the thermodynamic equilibrium conversion. Coal-based feed gas is likely to have considerably greater sulfur concentrations than those encountered in current WGSR processes, which use feed stocks derived from natural gas. Consequently, the search for catalysts that overcome these inherent problems, that is, the search for single-step low-temperature (LT) shift catalysts that are efficient and sulfur-tolerant, is an important part of coal gasification research.

Several reports in the literature suggest that homogeneous catalysis of WGS is highly active at LT and sulfur-tolerant. Catalysts active at temperatures as low as 60°C are reported to remain active in the presence of large sulfur concentrations. However, these studies were conducted in batch reactors with activities measured far from equilibrium. Those conditions are very different from industrial conditions of continuous operation close to equilibrium. The purpose of this project was to evaluate these homogeneous WGS catalysts under more industrially relevant conditions and to preliminarily compare the economics of a process based on high-activity, LT, sulfur-tolerant, homogeneous WGS catalysts to a process based on current industrial practice.

From this evaluation, we conclude that homogeneous catalysts do show activity at low temperature with good sulfur tolerance under industrially significant reaction conditions. The preliminary economic evaluation shows that the activities observed for these catalysts might offer, under certain conditions, economic advantage over current industrial practice. However, several economic and technical questions remain to be answered.

The DOE must decide what level of cost savings would be necessary to continue the development effort. If the goal of this program was to make hydrogen from coal competitive with current hydrogen from natural gas sources,we are far from that level. Current prices of hydrogen from natural gas are running $735 per metric ton.[98] If however the goal of this effort is to have the best available technology ready for the day when it becomes necessary to produce hydrogen from coal or to have the most cost effective route to hydrogen from coal available to integrate into an advanced coal liquefaction plant, then the homogeneous route is worth pursuing.

CONTENTS

LIST OF FIGURES

LIST OF TABLES

INTRODUCTION

In the long-term planning for energy resources and chemical feedstocks, hydrogen derived from steam gasification of coal may become an important alternative to hydrogen obtained from steam reforming of natural gas. The production of additional hydrogen from syngas by the water-gas shift reaction (WGSR) substantially enhances the yield of this product. Thus, a potentially important route to improving the economy of hydrogen production, particularly from coal, is to enhance the efficiency of industrial WGSR catalysis.

In current practice, syngas is shifted by passage through two sequential, heterogeneous, catalytic reactors.[1] The first operates at about 350°C, using an iron-chromia or cobalt-molybdenum catalyst that is resistant to sulfur poisoning (high temperature shift or HTS). At this temperature, the equilibrium conversion of CO to H_2 cannot exceed about 85% (Figure 1). After acid gas removal, the partially shifted gas is passed through a second reactor that contains, typically, a copper/zinc oxide catalyst at about 250°C (low temperature shift or LTS). Under these conditions, CO conversion can exceed 95%. Finally, the CO_2 produced in the second stage is removed from the product gas. The LTS is not suitable alone because the reaction is too slow over these catalysts and they typically are not sulfur-tolerant.

In contrast, a single homogeneous WGSR reactor can operate at temperatures below 200°C with equilibrium CO conversions to hydrogen exceeding 95%. Thus, provided that the rate of reaction is fast enough under these conditions, a single, homogeneous WGSR stage could replace the two-stage heterogeneous WGSR system. Furthermore, in this process scheme a homogeneous WGSR catalyst that exhibits high tolerance to sulfur would allow sulfur removal to be combined with the CO_2 removal step that is situated downstream from the WGSR. Reports in the scientific and patent literature[2,3] indicate that a number of homogeneous catalytic systems are capable of catalyzing the WGSR with moderate activity and, in some cases, with tolerance to sulfur and nitrogen feedstock impurities. These catalysts have not typically been examined with "practical" considerations in mind that is, under the constraints imposed by an industrial process. The activity of these catalysts has typically been evaluated in batch reactors

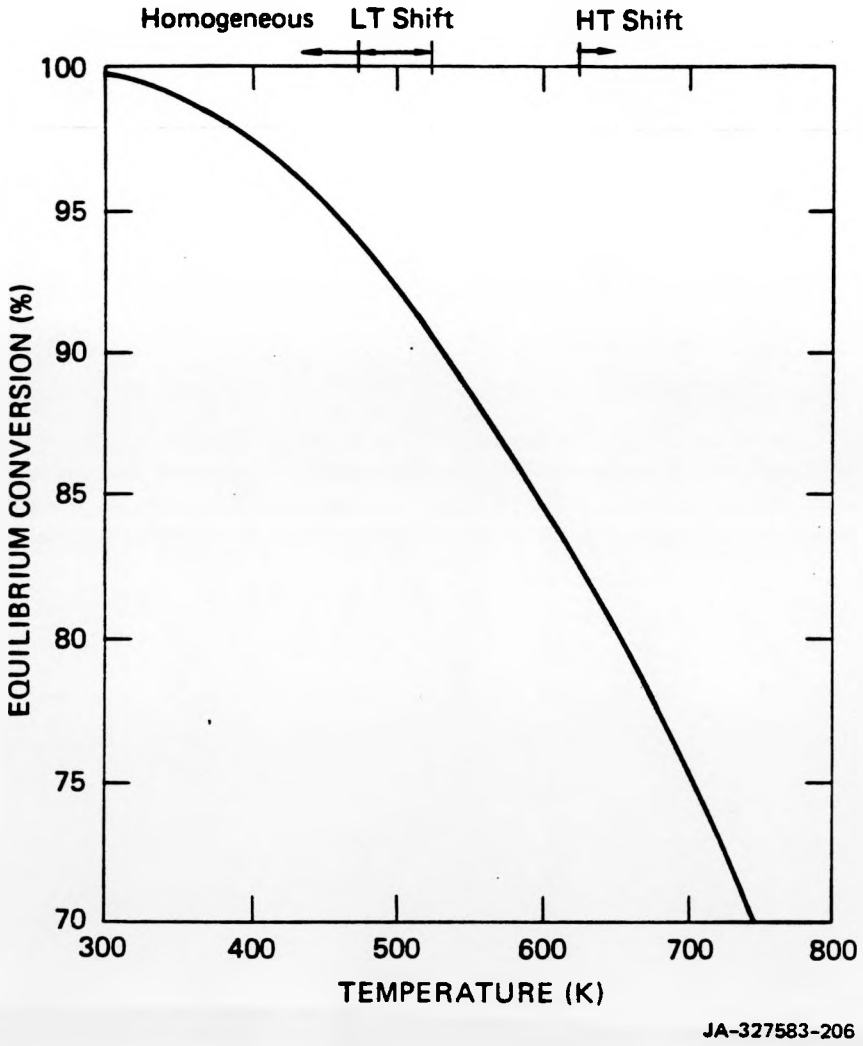

FIGURE 1. Equilibrium conversion of CO and H_2O to CO_2 and H_2 by WGS reaction at different temperatures.

Feed gas composition: 50% CO, 50% steam.

starting far from equilibrium, whereas in practice, continuous operation will be required using gas from an oxygen-blown gasifier as feedstock. That feed stock will already contain significant concentrations of hydrogen and carbon dioxide.

Considering the advantage of high equilibrium conversions at low temperatures using a catalyst that is sulfur-resistant, together with the process simplifications that accompany a single-stage reactor, it is evident that the homogeneous catalytic WGSR process offers great potential for significant savings in capital and operating costs. Therefore, we have evaluated the WGSR performance of selected homogeneous catalyst systems with simulated coal gas feedstocks for use in the production of hydrogen from coal gas. However, it is not obvious what kind of performance would be required to make the single-stage homogeneous WGSR process competitive with the currently practiced technology. Therefore, we also evaluated the impact of a single -stage homogeneous WGSR process on the economics of a hypothetical 1000-ton/day coal-to-hydrogen plant.

OBJECTIVE AND APPROACH

OBJECTIVE

The objective of this project was to identify, prepare, test, characterize, and evaluate a practical, homogeneous catalyst for a water-gas shift process. The effort was divided into the following five tasks:

(1) Update SRI's recent review of the literature on the catalysis of the water-gas shift reaction (WGSR) to include references after 1982 and those in the patent literature. Based on this review, SRI chose ten candidate systems to be evaluated as to their abilities to catalyze the WGSR using syngas derived from gasified coal.

(2) Develop a test plan designed to effectively evaluate both the catalysts and, to some extent, reactor configuration for WGSR catalysis.

(3) Perform a series of experiments to identify the most effective and economical of the ten candidate catalysts and then further evaluate the reaction kinetics of at least one selected catalyst system to develop sufficient data to provide the basis for the work in Task 4.

(4) Develop a mathematical model of the final candidate system that uses rate expressions to describe the catalytic process.

(5) Perform a technoeconomic evaluation of the catalyst in terms of a proposed plant design based on the reaction model, current costs, and standard chemical engineering practice and compare the proposed design with a conventional hydrogen plant.

Test Plan for Selection of Optimum Catalyst System

Based on the literature review, the following ten catalyst systems were selected to serve as candidates for further evaluation:

1	$Cr(CO)_6$/alcohol/base
2	$Mo(CO)_6$/alcohol
3	$W(CO)_6$/alcohol/base
4	$Ru_3(CO)_{12}$/alcohol/hydroxide
5	Ru/amine
6	$Fe(CO)_5/Ru(O)_{12}$/amine
7	Sulfonated rhodium/phenanthroline
8	Ruthenium/phenanthroline
9	Cobalt/phenanthroline
10	Meta-monosulfonated triphenyl phosphine/Rh

These systems were screened for water-gas shift reaction (WGSR) performance in a stirred, pressurized, batch reactor (Parr bomb), using the uniform initial experimental conditions specified in Table 1. These conditions (relatively high temperature, low H_2S concentration, and a long duration) were selected to be as favorable as possible for the WGSR, within the process constraints specified by DOE. A simulated coal gas feedstock representative of a Texaco gasifier operating in the oxygen-blown mode was used for this screening. This gas composition (Table 2) provides a high CO/CO_2 ratio that will realistically evaluate the performance of these catalysts close to equilibrium.

Table 1. SCREENING TEST CONDITIONS

Parameter	Initial Test
Pressure	25 atm
Temperature	450 K
Solvent	Diethylene glycol (or other high boiling solvent)
Feedstock	O_2-blown coal gas
Feedstock sulfur	1000 ppm H_2S
Duration	20 h

Table 2. FEEDGAS COMPOSITION

(Simulant of Coal Gas from Texaco Oxygen-Blown Gasifier)

Component	Volume Percent
H_2	22.0
CO	34.5
CO_2	7.0
H_2O	36.0
CH_4 or inert	0.5

The outcome of this screening process was the selection of two catalysts that have the following characteristics:

- WGSR activity
- Sulfur tolerance
- Low cost
- Compatibility with coal gas feedstock.

These catalysts were then studied under a variety of process conditions using a continuous-flow reactor. The data from the continuous-flow reactor were then used for a preliminary process economic evaluation (Task 5).

EXPERIMENTAL APPARATUS AND PROCEDURE

Screening Test

Screening tests were performed in a stirred batch reactor at elevated pressure. The reactor, a 45-cm^3 PTFE-lined Parr bomb containing a magnetic stir bar, is incorporated into a pressurizing and sampling system that withdraws and analyzes small portions of the reactor contents in accordance with a predetermined program. Analyses for CO and CO_2 are performed by a Hewlett-Packard 5880 gas chromatograph equipped with a Poropak Q or T column and a thermal conductivity detector. The system is shown schematically in Figure 2. After being filled with the solvent-catalyst solution, the bomb is closed and placed above the preheated temperature-controlled oil bath. The magnetic stirrer is activated

and premixed. Simulated coal gas is admitted to bring the pressure to the desired level, and the preheated oil bath is raised to immerse the bomb and start the reaction. The microprocessor on the gas chromatograph is programmed to actuate a two-valve sampling configuration at specified time intervals (Figure 2). Operation of the first valve A, fills a 0.05-μL sample volume internal to valve B with gas from the reactor. Before another sample is injected, the sample volume is purged with solvent or dry gas by actuation of valve 1.

Because the initial test runs were for 20 hours, they extended overnight. During this time, the fractional conversion of CO was measured and recorded automatically in accordance with the programmed schedule. These data provided a measure of the rate of the WGSR on the catalyst under the imposed conditions of temperature, pressure, and sulfur contamination.

Continuous-Flow Reactor

The experiments performed in the batch reactor system used for the screening tests provide several clues to the WGSR mechanism. These include overall rate of conversion of CO, some insight into the effect of pressure and temperature on rate, and the role of the solvent in the process. For measurement of reaction kinetics, however, a differential flow reactor is more appropriate because it operates in a steady-state mode and it is capable of accurately measuring higher rates. Such a reactor can be operated either in tubular-flow (TFR) or continuously stirred tank (CSTR) mode. To operate a TFR under differential conditions would require the precise measurement of small changes in the concentration of reactant between the fed and effluent streams. In a CSTR, however, relatively large changes in concentration between feed and effluent can occur in the absence of concentration gradients within the catalyst bed. In the ideal CSTR (back mix reactor), the composition and concentrations in the effluent are identical to those inside the catalyst bed. A well-stirred, internal recycle reactor approaches the ideal CSTR when the ratio of recycle rate to feed flow rate is high.

Figure 3 shows a general diagram of the reactor system that we used for these continuous-flow studies. The flow rate of the simulated coal gas mixture into the 300-mL autoclave is controlled by a Brook's mass flow controller that has been calibrated with a flowmeter; a linear plot of flow controller reading versus flowmeter reading had a correlation coefficient value of 0.99996. A known amount of water is mixed with this feedgas stream before it enters the reactor by using a high pressure metering pump and vaporizer. The reaction mixture is stirred with a Dispersimax stirrer at about 2200 rpm to

ensure adequate mixing of the gas within the reaction solution. The gas lines from the vaporizer to the chromatograph were heated to a minimum temperature of 150°C; in later runs this minimum was raised to 180°C to prevent condensation in the output lines. The output gases from the reactor flow continuously to a vent via a back pressure regulator, a multiport Valco valve, and a sample loop, which automatically injects a sample at regular intervals into an HP 5880A gas chromatograph.

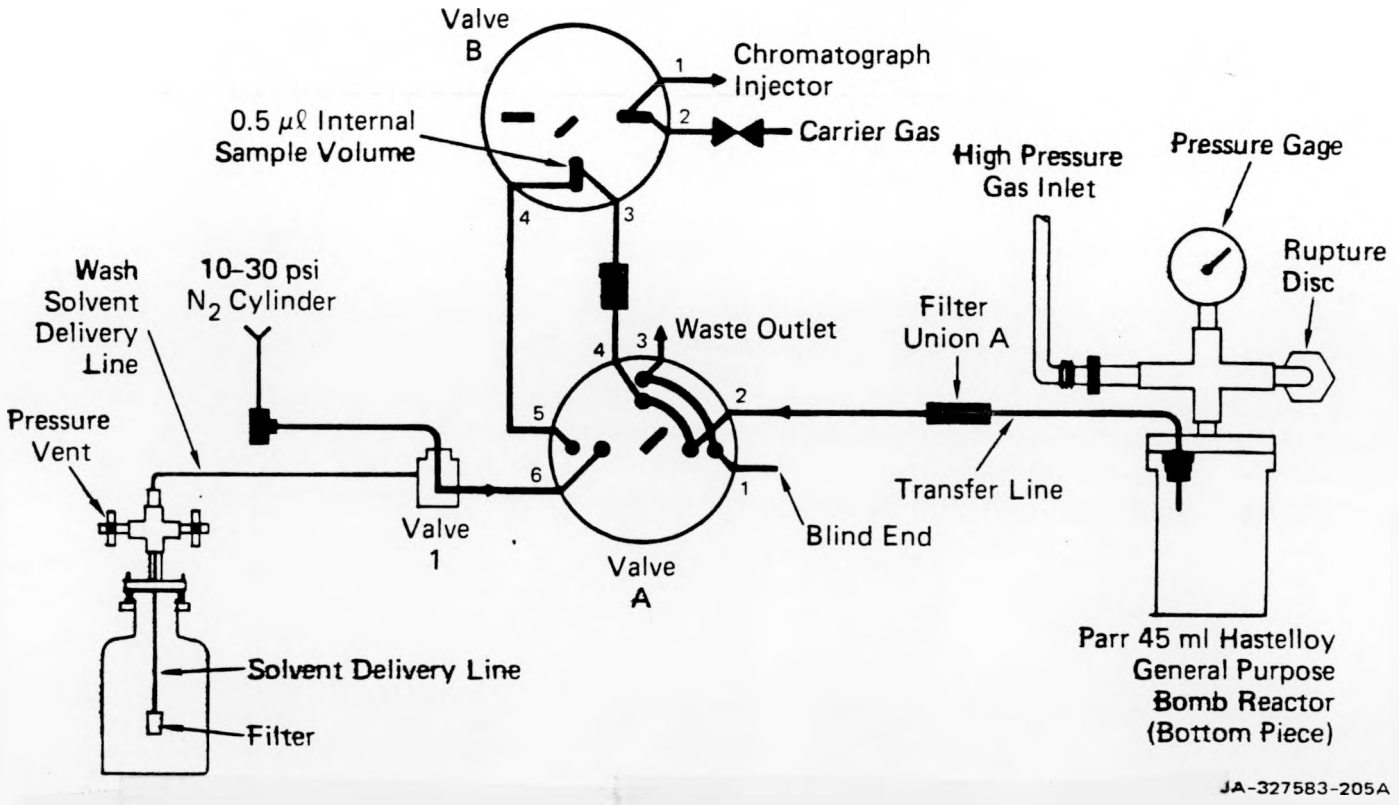

FIGURE 2. High pressure, high temperature automatic sampling reactor system.

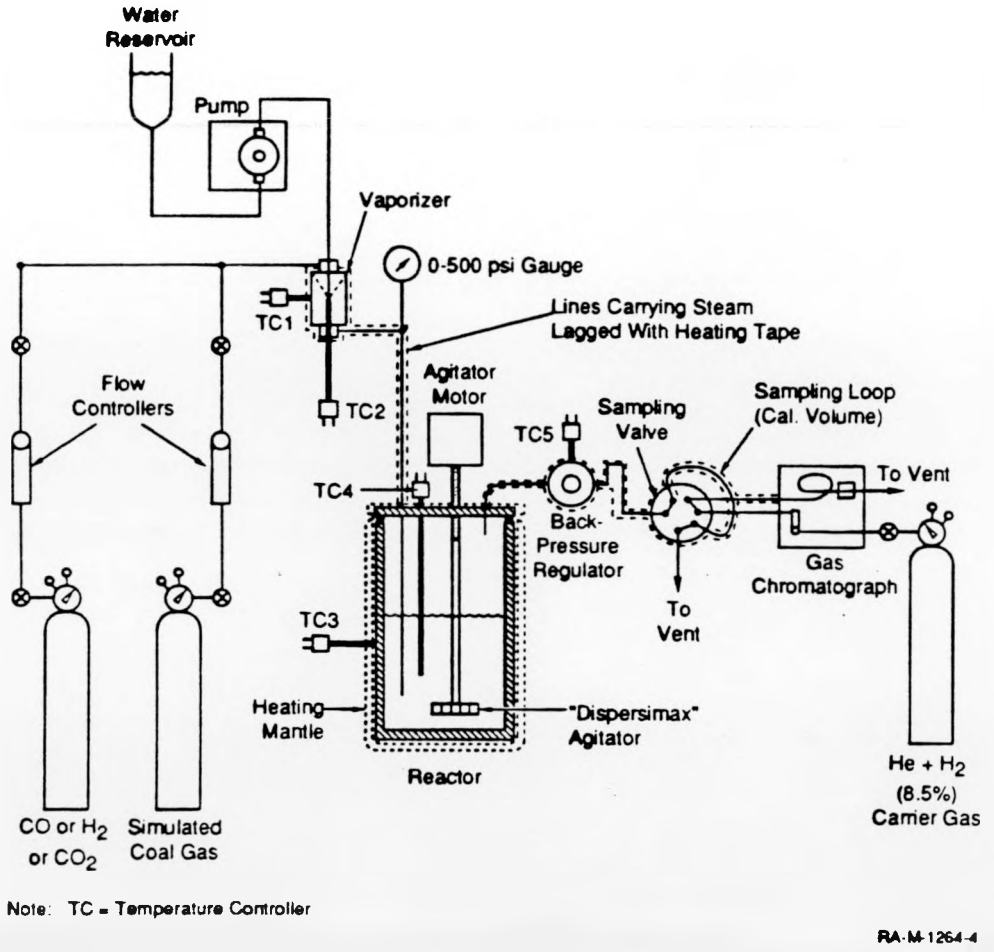

FIGURE 3. Continuous-flow reactor with recycle for the homogeneous WGSR.

BACKGROUND

This background is drawn from two review papers published by SRI.[2,3]

The first research on the possibility of homogeneous catalysis of the WGSR was reported by Reppe.[4] Reppe's work with catalytic reactions of the general form shown in reaction (1)

$$CO + H_2O + S \xrightarrow{\text{catalyst}} SH_2 + CO_2 \qquad (1)$$

S = substrate (such as aldehyde or olefin)
catalyst = $Fe(CO)_5$ or $Ni(CO)_4$

led him to postulate that a process akin to catalysis of the WGSR was occurring. However, it was only in the early 1970s that the first examples of homogeneous catalysis of the WGSR appeared in the patent literature and then in the open literature. Fenton was the first to describe homogeneous catalysis of the WGSR, in three patents,[5-7] by a variety of group 8 metals stabilized with phosphine, arsine, or stibine ligands and requiring amine or inorganic bases as promoters or cocatalysts.

In the same time period, the first reports on the homogeneous catalysis of the WGSR appeared in the open literature. Four types of catalyst systems were identified initially. Laine et al. reported that aqueous alcoholic solutions of ruthenium carbonyl made basic with KOH gave active WGSR catalyst systems.[8] Kang et al. were able to show that the majority of the group 8 metal carbonyls were active catalysts for the WGSR when dissolved in aqueous THF containing trimethylamine as base.[9] In contrast, Cheng et al. demonstrated that it was possible to catalyze the WGSR in acidic solution.[10] Rhodium carbonyl complexes in aqueous acetic acid containing iodide gave active WGSR catalysts. Likholobov et al. reported, at approximately the same time, the discovery of a palladium phosphine WGSR catalyst system that requires aqueous trifluoroacetic acid as the working medium.[11] The initial evidence suggested that the two base-promoted catalytic cycles were similar, but differed mechanistically from the acid-facilitated systems.

From these original reports, as well as the mechanistic evidence presented later by other research groups, it is evident that there are a variety of catalytic cycles possible for homogeneous catalysis of the WGSR (see, for example, the recent review by Ford[12]). In general, the various types of catalytic cycles proposed for the WGSR can be distinguished according to whether CO or H_2O activation occurs in the primary step and whether catalysis occurs under acidic, basic, or neutral conditions. Other distinguishing features include the presence or absence of ligands other than CO or H_2O and the use of group 6 or 8 metal complexes. Because so many mechanisms for catalysis of the WGSR have been proposed in the literature, we have organized our discussions in terms of the types of mechanisms described or proposed to date.

Before discussing the individual mechanisms for specific systems studied, we describe the variations possible in the basic chemistry associated with WGSR catalytic cycles. These discussions will allow the reader to compare and contrast the chemistry presented in the various catalytic cycles that follow.

FUNDAMENTAL STEPS IN WGSR CHEMISTRY

The majority of the WGSR systems described in the literature are initiated by activation of CO followed by its reaction with water, OH^-, or H_3O^+. The less well-studied systems start with activation of H_2O, followed by reaction with CO. We will begin our discussions by considering catalytic cycles that begin with CO activation.

Carbon monoxide activation normally starts with complexation of free CO to a coordinately unsaturated metal. Once bound, the carbonyl's reactivity toward water, OH^-, or H^+ is determined by the extent to which it π backbonds to the metal, the metal's oxidation state, the overall charge on the complex, and the extent to which the complex can stabilize the various possible intermediates that could form following reaction with water, base, or acid.

When the metal has considerable electron density to donate back to the coordinate CO group, nucleophilic attack is suppressed. In fact, high electron density at the metal can have a dramatic adverse effect on nucleophilic attack at CO. For example, Gross and Ford observe that the substitution of a single phosphite group onto $Ru_3(CO)_{12}$ reduces its reactivity toward CH_3O^- by approximately two orders of magnitude.[13] Complexes with high electron density include anionic complexes and neutral complexes of low valent metals supporting several good electron donor ligands.

When the nucleophile is OH^-, the product will be an anionic metallocarboxylic acid, reaction (2).

$$MCO + OH^- \longrightarrow M(CO_2H)^- \qquad (2)$$

In contrast, when the metal has little electron density to donate to the coordinated CO, as occurs when the metal is in a high oxidation state or the overall complex is positively charged, then even weak nucleophiles such as H_2O can react with the CO, reaction (3), to produce a metallocarboxylic acid.

$$MCO^+ + H_2O \longrightarrow M(CO_2H) + H^+ \qquad (3)$$

This reaction has been used by several researchers as a facile way of labeling carbonyl oxygens:[14-16]

$$Re(CO)_6\,S + H_2O \longrightarrow (CO)_5Re[C(=O)^*OH]^+$$

$$\longrightarrow (CO)_5Re[C(=^*O)OH]^+ \longrightarrow (CO)_5Re(C^*O)^+ + H_2O \qquad (4)$$

An alternative reaction pathway is available for CO bound to a relatively electron-rich metal. It is quite reasonable that under acidic conditions the entire complex can be protonated. Protonation reduces the electron density available for backbonding with the CO, making it sufficiently electron-deficient that it can then react with water, as illustrated in reaction (5), to form a metallocarboxylic acid.

$$MCO + H^+ \longrightarrow HMCO^+ + H_2O \longrightarrow HM(CO_2H) + H^+ \qquad (5)$$

For acidic reactions, the introduction of strong electron donor ligands should have the opposite effect to that observed with the nucleophilic reactions; it should promote the reaction of H^+ with MCO. However, there is no evidence to support this idea at present.

An additional route to CO activation that does not rely on initial complexation with a coordinately unsaturated metal begins with the reaction of CO with OH^- to produce formate and reaction with excess water to produce formic acid:

$$CO + OH^- \longrightarrow HCO_2^- \quad (6)$$

$$HCO_2^- + H_2O \longrightarrow HCO_2H + OH^- \quad (7)$$

The formate anion or formic acid can then bind to a coordinately unsaturated metal to form a metalloformate rather than a metallocarboxylic acid:

$$M + HCO_2H \longrightarrow HM(\eta^1 \text{ or } \eta^2\ O_2CH) \quad (8)$$

$$M + HCO_2 \longrightarrow [M(O_2CH]^- \quad (9)$$

Metal formates could also arise via rearrangement of a metallocarboxylic acid, as shown in reactions (10) or (11):

$$M(CO^2H) \longrightarrow [HM(\eta^2\text{-}CO^2)] \longrightarrow M(O_2CH] \quad (10)$$

$$HM(CO_2H) \longrightarrow M + HCO_2H \longrightarrow HM(O_2CH) \quad (11)$$

The existence of metallocarboxylic acids and evidence for their formation upon reaction of carbonyls with OH^- are now well established, beginning with the initial report by Deeming and Shaw[17] and continuing with the more recent work of Gross and Ford,[13]

Darensbourg and Rokicki,[18-19] Lane et al.,[20] and others. The following complexes have been isolated and/or identified spectroscopically:

$IrCl_2(CO_2H)(CO)(PMe_2PH)_2$ (Ref. 17)

$CpFe(CO)(PPh_3)CO_2H$ (Ref. 21)

$CpRu(CO)(PPh_3CO_2H$ (Ref. 22)

$(Et_3P)_2Pt(Cl)CO_2H$ (Ref. 23)

trans-$PtH(CO_2K)[P(iPr_3)_3]_2$ (Ref. 24)

$CpRe(NO)(CO)CO_2H$ (Ref. 25)

$Mn(CO)_5CO_2H$ (Ref. 18)

$Ru_3(CO)_{11}CO_2H$ (Ref. 13)

$Fe(CO)_4CO_2H^-$ (gas phase) (Ref. 20)

Metallocarboxylic acids could also arise via the formate pathway, reaction (6) [and ((7)], if the metal preferentially inserted into the formate (formic acid) C-H bond rather than forming a metalloformate:

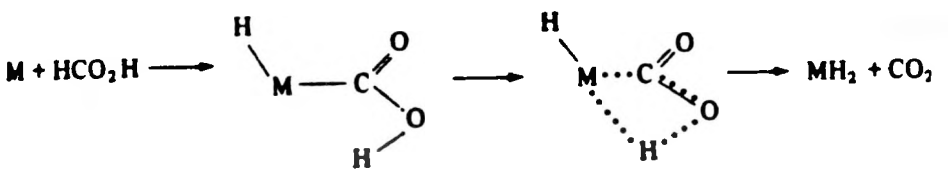

Scheme 1

Support for the reactions shown in Scheme 1 comes from the work of Grey et al.,[26] who find that $H_2Ru(C_6H_4PPh_2)(PPh_3)_2$ reacts with formate esters to give decarbonylation reactions. Presumably, these reactions are initiated by C-H insertion.

Although metalloformate complexes have been less well studied, the emphasis in the available publications has been with regard to the catalytic decomposition of formate and formic acid via metalloformate intermediates in WGSR catalysis. The formate or formic acid is assumed to be produced via reactions (6) and (7). For example, Darensbourg has described the preparation and characterization of a number of formate

complexes including $CpFe(CO)_2(O_2CH)$,[27] and the group 6 complexes $(HCO_2)M(CO)_5$[19] (where M = Cr, Mo, W).

Once the activated CO has reacted with water to give either a metallocarboxylic acid or a metalloformate, the possibility now exists for eliminating CO_2—one of the products of the WGSR. Deeming and Shaw[17] were the first to observe that metallocarboxylic acids can decompose with loss of CO_2, reaction (12).

$$IrCl_2(CO_2H)(CO)(PMe_2Ph)_2 \longrightarrow IrHCl_2(CO)(PMe_2Ph)_2 + CO_2 \quad (12)$$

In fact, the majority of the metallocarboxylic acids and metalloformates cited above decompose rather readily to produce CO_2 and a metal hydride; however, the exact mechanisms can vary. Originally, it was assumed that the decomposition process proceeds via beta elimination, as seen in reaction (13).

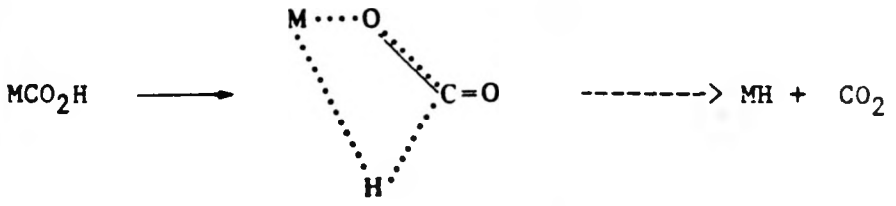

(13)

More recently, a number of groups have described decomposition processes in which catalytic amounts of base are required to promote decomposition. This requirement suggests that the metallocarboxylate anion, MCO_2^-, is a necessary intermediate in some decomposition processes:

$$MCO_2^- \longrightarrow CO_2 + M^- + H_2O \longrightarrow MH + OH^- \quad (14)$$

Three other bimolecular decomposition pathways have been proposed in the literature. Reactions (15) and (16) are suggested by the work of Darensbourg.[19,28]

$$MCO_2 + OH^- \xrightarrow{[MC(OH)_2O^-]} MH + OH^- \quad (15)$$

$$MCO_2H + H_2O \xrightarrow{[MC(OH)_2O^-]} MH + H_2CO_3 \quad (16)$$

Reaction (17) is suggested by the work of Gibson and Ong:[22]

$$MCO_2H + MH \longrightarrow H_2 + M_2 + CO_2 \quad (17)$$

Unfortunately, quantitative studies of the decomposition kinetics of metallocarboxylic acids are quite limited, and thus the mechanisms of decomposition must remain at least partly conjecture.

Reaction (18) is another decomposition pathway available to metallocarboxylic acids:

$$MCO_2H \xrightarrow{[M(OH)CO]} MOH + CO \quad (18)$$

however, this decomposition process is counterproductive in a WGSR sense, because it leads back to reactants rather than to products. Grice et al. report[21] that in some solvents $CpFe(CO)^+$ reacts reversibly with OH^- as shown in (18), but can be coerced into undergoing decarboxylation by changing solvent and adding base. Therefore, some control over the dominant mechanism in metallocarboxylic acid decomposition is possible.

Metalloformate intermediates decarboxylate to give essentially the same products as obtained from decomposition of metallocarboxylic acids; consequently, it is likely that in some WGSR catalysis systems it will not be possible to distinguish between two similar catalytic mechanisms.

As noted above, metalloformates are proposed intermediates in the catalytic decomposition of formate and formic acid formed as per reactions (6) and (7). The general reactions for these decompositions can be written as in reactions (19) and (20).

$$M^{+}O_2CH^{-} \xrightarrow{[M(O_2CH)]} MH^{-} + CO_2 \qquad (19)$$

$$M + HCO_2H \xrightarrow{[HM(O_2CH)]} M + H_2 + CO_2 \qquad (20)$$

The formation and decomposition of transition metal formate complexes have been discussed as part of a review by Eisenberg and Hendriksen.[29]

A number of metal complexes have been reported to promote reaction (20) catalytically. Strauss et al. report[30] that $Rh(C_6H_4PPh_3)_2$ catalyzes (20) and compare the activity of this catalyst with the activities of $Pd(HCO_2)_2$, $PtCl_2(PBu_3)_2$, $IrH_2Cl(PPh_3)_3$, and $Pt[P(iPr)_3]_3$. The platinum isopropylphosphine complex appears to have the highest activity of the catalysts compared. Other compounds, including $Ru_3(CO)_{12}$ and $Ir_4(CO)_{12}$,[12,31] have also been found to be active catalysts for (20).

Metalloformates such as the intermediate shown in (20) can also be isolated in the reversible reaction between metal hydrides and CO_2 as exemplified by reaction (21):[32]

$$PtH_2(PEt_3)_2 + CO_2 \rightleftharpoons (HCO_2)PtH(PEt_3)_2 \qquad (21)$$

The reversible reaction of CO_2 with metal hydrides to form metalloformates is important to the current discussion because such a reaction, e.g. (21), is potentially counterproductive in a WGSR sense, because it ties up metal hydride and CO_2 as metalloformate, preventing release of both H_2 and CO_2. This potential problem is particularly important in WGSR catalysis by group 6 metal catalysts, as discussed below.

The mechanism of η-1 or η-2 formate decomposition is generally assumed to be one that involves a beta elimination process:

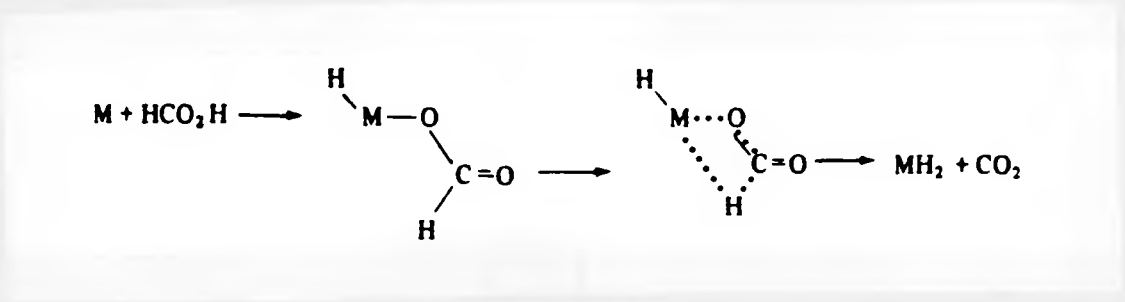

Scheme 2

One other organometallic source of CO_2 was described by Yoshida et al.,[33] who report that selected rhodium phosphine complexes (see below) undergo a reaction sequence in which reaction (16) is followed by reactions (22) and (23).

$$MH + H_2CO_3 \longrightarrow H_2 + M(O_2COH) \qquad (22)$$

$$M(O_2COH) \longrightarrow M^+ + OH^{-2} + CO_2 \qquad (23)$$

In the preceding paragraphs, we have discussed the potential organometallic intermediates that can activate CO and promote its reactions with H_2O; we have also examined the potential intermediates available for the evolution of the WGSR product, CO_2. The following discussions provide a similar treatment of how H_2 evolution, the other WGSR product, can result from organometallic complexes such as MH, the likely by-product of CO_2 formation.

Unimolecular reductive elimination provides the simplest possible route for generation of H_2:

$$MH_2 \longrightarrow H_2 + \text{"M"} \qquad (24)$$

Kinetic studies have shown that a number of complexes, including $H_2Fe(CO)_4$,[34] $H_2RhCl(PPh_3)_3$,[35] $H_2IrCl(CO)(PPh_3)_2$,[36] and $H_2Co[P(OR)_3]_4$,[37] eliminate H_2 by unimolecular reductive elimination. H_2 can also be formed through bimolecular elimination

reactions [e.g., (25)] as shown by Marko and Ungvary for $HCo(CO)_4$[38] and by Norton for $H_2Os(CO)_4$:[39]

$$MH + MH \longrightarrow M_2 + H_2 \quad (25)$$

$$2HCo(CO)_4 \longrightarrow Co_2(CO)_8 + H_2 \quad (26)$$

$$2H_2OOs(CO)_4 \longrightarrow H_2Os_2(CO)_8 + H_2 \quad (27)$$

In most instances, bimolecular loss of H_2 requires an initial dissociative step in which creation of a coordinately unsaturated species [e.g., $HCo(CO)_3$ in (26)] permits the formation of a bridging hydride intermediate, which then leads to H_2 and a dimeric species. In the case of $H_2Fe(CO)_4$, the process is further complicated by competing multinuclear processes, which provide additional routes for reductive elimination of H_2, as demonstrated by Collman et al.[40]

$$H_2Fe(CO)_4 + Fe(CO)_4 \longrightarrow H_2Fe_2(CO)_8 \quad (28)$$

$$H_2Fe_2(CO)_8 + HFe_2(CO)_8^- \longrightarrow HFe_3(CO)_{11}^- + Fe(CO)_5 + H_2 \quad (29)$$

In the analogous ruthenium systems, it appears that multinuclear H_2 elimination processes are the only pathways available.[41]

$$3[H_3Ru_4(CO)_{12}]^- + 9CO \longrightarrow 3[Ru_3(CO)_{11}]^- + Ru_3(CO)_{12} + 3H_2 \quad (30)$$

Alternative paths will be discussed when the ruthenium system is discussed in detail later in this section.

Reactions (24)-(30) illustrate only that portion of known organometallic chemistry where H_2 formation proceeds via reductive elimination from metal hydrides. Alternative mechanisms are available for H_2 production that do not proceed via reductive elimination. For example, metal hydrides are known to react with acids according to reaction (31):

$$MH + HX \longrightarrow MX + H_2 \qquad (31)$$

Reactions (32)-(35) provide specific examples of reaction (31) in which MH is an organometallic hydride:[42a]

$$CpFe(CO)_2H + HCl \longrightarrow CpFe(CO)_2Cl + H_2 \qquad (32)$$

$$Cp_2ZrH_2 + HOAc \longrightarrow Cp_2Zr(OAc)_2 + H_2 \qquad (33)$$

$$\text{mer-}HIrCl_2(PPh_3)_3 + HCl \longrightarrow \text{mer-}IrCl_3(PPh_3)_3 + H_2 \qquad (34)$$

$$Pd[P(Ph)_3]_4 + 2HX + H_2O \longrightarrow Pd(H_2O)[P(Ph)_3]_3X_2 + P(Ph)_3 + H_2 \qquad (35)^{42b}$$

It is likely that transition metal hydrides will undergo similar reactions when $HX = H_2O$.

Bricker et al.[41,43] have suggested another mechanistic process leading to H_2 evolution. Given that metal formyl complexes are very efficient hydride donors and, based on the rationale by Pearson et al.[34b] that metal formyls can form under mild conditions (recently supported by the theoretical work of Blyholder et al.[44]), Bricker et al.[43] propose reaction (36) as a plausible source of H_2:

$$MC(=O)H + H_2O \longrightarrow M(CO)^+ + OH^- + H_2 \qquad (36)$$

Unfortunately, it may not be possible to distinguish between reaction (31), where $HX = H_2O$, and reaction (36).

In contrast to the work on WGSR processes wherein the first step is CO activation, there are very few examples where metal-promoted activation of water precedes reaction with CO. As seen in reactions (37)-(39), the overall WGSR mechanisms that begin with H_2O activation are quite similar to those beginning with CO activation.

$$M + H_2O \longrightarrow HM(OH) \quad (37)$$

$$HM(OH) + CO \longrightarrow [HM(CO)(OH)] \longrightarrow HM(CO_2H) \quad (38)$$

$$HM(OH) + CO \longrightarrow HMCO + OH^- \longrightarrow HM(CO_2H) \quad (39)$$

In reality, it appears that the specific factors that cause the differentiation between H_2O and CO activation apply only for the first step in the WGSR catalytic cycle.

The key features that appear to facilitate water activation rather than CO activation are simultaneous, high coordinative unsaturation and high electron density at the metal as found in $Pt[P(iPr)_3]_3$,[45] $Rh[P(iPr)_3]_3$,[46] and $W((CO)_3(PCy_3)_2$.[47] These compounds react with water to give trans-$PtH(OH)[P(iPr)_3]$, $HRh(OH)[P(iPr)_3]_3$, and $HW(OH)(CO)_3(PCy_3)$. Under these circumstances, it seems reasonable to suggest that oxidative addition of H_2O is preferred to CO coordination because it reduces both electron density and coordinative unsaturation significantly more than what can be attained with CO coordination. Only the platinum and iridium complexes have been shown to react with CO to form metallocarboxylic acids and to catalyze the WGSR as discussed below.

The various possible WGSR reaction intermediates described above serve as the basis for the following detailed discussions on the reported examples of homogeneous catalysis of the WGSR. These examples are separated into two groups: catalysis of the WGSR under basic conditions and catalysis under acidic or neutral conditions.

CATALYSIS OF THE WGSR UNDER BASIC CONDITIONS

Iron Carbonyl Catalysis

Perhaps the simplest WGSR catalyst system studied to date is the system based on $Fe(CO)_5$. The first reports on a base-promoted catalyst system were made by Kang et al.[48]

and King et al.[49] Kang et al. described studies using a $Fe(CO)_5$, $Me_3N/THF/H_2O$ WGSR system. King et al. studied WGSR catalysis by aqueous alcoholic solutions of $Fe(CO)_5$ made basic with alkali metal hydroxides.

King et al. have since continued their studies[50] on the hydroxide-promoted systems; based on high temperature IR data and the work of Kang et al., they propose the mechanism shown in Scheme 3.

$$Fe(CO)_5 + OH^- \longrightarrow Fe(CO)_4C(=O)OH^-$$

$$Fe(CO)_4C(=O)OH^- \longrightarrow HFe(CO)_4^- + CO_2$$

$$HFe(CO)_4^- + H_2O \longrightarrow H_2Fe(CO)_4 + OH^-$$

$$H_2Fe(CO)_4 \longrightarrow H_2 + Fe(CO)_4$$

$$Fe(CO)_4 + CO \longrightarrow Fe(CO)_5$$

SCHEME 3

King et al. report that the rate-determining step in the catalytic cycle is the reaction of base with $Fe(CO)_5$, which was confirmed by Pearson and Mauermann.[34] From kinetic studies of these same systems, Pearson and Mauermann show that loss of CO_2 proceeds via deprotonation of the metallocarboxylic acid rather than directly from the metallocarboxylic acid:

$$Fe(CO)_4CO_2H^- \longrightarrow [Fe(CO)_4(CO_2)]^{2-} \qquad (40)$$

$$[Fe(CO)_4(CO_2)]^{2-} + H_2O \longrightarrow HFe(CO)_4^- + HCO_3^- \qquad (41)$$

In support of reactions (40) and (41), Lane et al.[20] report that $Fe(CO)_4CO_2H^-$ is stable to decarboxylation in the gas phase even in the presence of added water molecules or unsolvated secondary bases. However, they do find that the addition of the hydroxide/ammonia cluster ion $(OH)NH_3^-$ promotes decarboxylation of $Fe(CO)_4CO_2H^-$ as

in (40). Lane et al. also calculate that the lower limit to the enthalpy of decarboxylation is approximately -17 kcal/mol. This points up a continuing problem in WGSR catalysis studies, namely, the extreme dearth of thermodynamic data needed both to differentiate between various possible mechanistic pathways and to calculate the potential efficiencies of new WGSR catalyst systems.

Contrary to the work of Pearson and Mauermann and of Lane et al., recent kinetic studies by Gross and Ford[13] on the $Fe(CO)_5/OH^-$ system in mixed THF/MeOH/H_2 solvent systems indicate that decarboxylation proceeds via the metallocarboxylic acid, $Fe(CO)_4C(=O)OH^-$, rather than via the dianion as in reaction (40). The evidence suggests that protic media catalyze the decarboxylation step.[51]

Ruthenium Carbonyl Complexes

Since the original reports on ruthenium catalysis of the WGSR in 1977,[8] this system has been the subject of considerable study by the original discoverers as well as by many other groups in the field. The currently proposed mechanism, shown in Scheme 4, can be derived from the work of Gross and Ford[13] and of Bricker et al.[43]

$$Ru_3(CO)_{12} + OH^- \longrightarrow Ru_3(CO)_{11}(CO_2H)^-$$

$$Ru_3(CO)_{11}(CO_2H)^- \longrightarrow CO_2 + HRu_3(CO)_{11}^-$$

$$HRu_3(CO)_{11}^- + CO \longrightarrow [HRu_3(CO)_{12}^-]$$

$$[HRu_3(CO)_{12}^-] + H_2O \longrightarrow Ru_3(CO)_{12} + H_2 + HO^-$$

$$HRu_3(CO)_{11}^- + H_2 \longrightarrow H_3Ru_4(CO)_{12}^- + CO$$

$$H_3Ru_4(CO)_{12}^- + CO \rightleftharpoons HRu_4(CO)_{12}^- + H_2$$

$$HRu_4(CO)_{12}^- + CO \rightleftharpoons HRu_3(CO)_{11}^- + Ru_3(CO)_{12} + H_2$$

SCHEME 4

Gross and Ford have presented concrete evidence for the intermediacy of the trinuclear cluster metallocarboxylic acid formed in Scheme 4. Moreover, the results of their

kinetic studies indicate that $Ru_3(CO)_{11}(CO_2H)^-$ is the intermediate that undergoes decarboxylation rather than the dianon, $Ru_3(CO)_{11}(CO_2)^-$. Bricker et al. provide convincing evidence that the reaction of $HRu_3(CO)_{11}^-$ with CO leads to hydrogen evolution by either of two pathways.[41]

In the absence of water, $HRu_3(CO)_{11}^-$ reacts reversibly with CO as in reaction (42):

$$K^+ + HRu_3(CO)_{11}^- + CO \rightleftharpoons Ru_3(CO)_{12} + KH \qquad (42)$$

Based on reaction (42), Bricker et al.[41] suggest that hydrogen evolution results from the formation of the intermediate or transient species, $HRu_3(CO)_{12}^-$. This species can lose hydride and generate H_2 either as in reaction (42), with subsequent hydrolysis of KH, or through formation of a formyl intermediate, $(CHO)Ru_3(CO)_{11}^-$, coincident with reaction (36). Bricker et al. also suggest that the two equilibria in Scheme 4, wherein tetranuclear species interconvert with trinuclear species, are side reactions that diminish the reactivity of the ruthenium WGSR catalyst system because they tie up metal in a nonproductive or less productive form.

Slegeir et al.[52] briefly studied several aspects of ruthenium catalysis of the WGSR using amine as base. Their studies with the $(CH_3)_3N/THF/H_2O$ solvent system suggest the following mechanism for amine-promoted WGSR catalysis.

$$Ru_3(CO)_{12} + 3CO \rightleftharpoons 3Ru(CO)_5$$

$$Ru(CO)_5 + (CH_3)_3N \rightleftharpoons (CO)_4Ru[C(=O)N(CH_3)_3]$$

$$(CO)_4Ru[C(=O)N(CH_3)_3] + H_2O \rightleftharpoons HRu(CO)_4^- + CO_2 + (CH_3)_3NH^+$$

$$HRu(CO)_4^- + H_2O \rightleftharpoons H_2Ru(CO)_4 + OH^-$$

$$H_2Ru(CO)_4 \rightleftharpoons H_2 + Ru(CO)_4$$

$$Ru(CO)_4 + CO \rightleftharpoons Ru(CO)_5$$

SCHEME 5

The evidence in support of this mechanism is not consistent. Slegeir et al.[52] find that, at higher $Ru_3(CO)_{12}$ concentrations, CO pressure dependence studies implicate clusters as the active catalyst species, and they isolate $H_4Ru_4(CO)_{12}$ by acidifying the reaction solution. At lower $Ru_3(CO)_{12}$ concentrations and CO pressures, they observe higher WGSR catalysis activity and conclude that mononuclear species are involved.

Two explanations for these observations are possible, both of which would discount the mechanism shown in Scheme 5. One is that the last two equilibria in Scheme 4 could readily account for the pressure/activity dependence data if trinuclear species are the true active WGSR catalyst species in amine-promoted ruthenium WGSR as they are in the hydroxide-promoted system. Then Scheme 4 rather than Scheme 5 provides the appropriate mechanism. The alternative, which we believe is more likely, is that strong amine cluster interactions change the nature of the catalyst entirely. This changed is evidenced by the disparity between the recorded amine- and OH^--promoted WGSR catalyst activities, especially for the Ru and Rh systems, as seen from a comparison of the data in Tables 3 through 5.

The work of Wilson and Laine[53] provides a possible explanation of these differences. In an effort to explain the reversal in relative activities of the two catalysts, Wilson and Laine have presented evidence that a majority of the second- and third-row group 8 metals interact strongly with tertiary amines through C-H activation, as evidenced by reaction (43) where the catalyst can be ruthenium, osmium, rhodium, or iridium carbonyl.

$$Et_3N + D_2O + CO \xrightarrow{\text{catalyst}} Et_2NCHDCD_3 + CO_2 + HD \qquad (43)$$

The fact that amine cluster complexes can be isolated from the catalyst solutions containing many types of amines suggests that the catalyst system is extremely complex. Thus, a simple explanation of the mechanisms of amine-promoted group 8 metal catalysis of the WGSR is not at present possible.

Table 3. HYDROXIDE-PROMOTED CATALYSIS OF THE WGSR

Catalyst	Solvent	Pressure CO (atm)	Temp. (°C)	Turnovers /24 h	Ref.
$Fe(CO)_5$	n-BuOH	28.2	137	16	49
$Fe(CO)_5$	n-BuOH	28.2	181	72	49
$Ru_3(CO)_{12}$	$EtOCH_2CH_2OH$	1	100	2.2	64b
$Ru_3(CO)_{12}$/ $Fe_3(CO)_{12}$	$EtOCH_2CH_2OH$	1	100	7.4	64b
$RuCl_3$	H_2O	0.33	90	3	55
$RuCl_3$	$H_2O/EtOCH_2CH_2OH$	0.33	90	1.4	55
$Ru_3(CO)_{12}$	MeOH	75	135	53	64b
$Os_3(CO)_{12}$	MeOH	75	135	12	64b
$Rh_6(CO)_{16}$	MeOH	75	135	110	64b
$Ir_4(CO)_{12}$	MeOH	75	135	17	64b
$Ir_4(CO)_{12}$	$EtOCH_2CH_2OH$	0.9	100	15	31
$Cr(OH)_6$	MeOH	7.8	140	280	49
$Mo(CO)_6$	MeOH	11	145	130	49
$W(CO)_6$	MEOH	7.8	130	140	49

Table 4. AMINE-PROMOTED CATALYSIS OF THE WGSR

Catalyst	Solvent /amine	Pressure CO (atm)	Temp. (°C)	Turnovers /10 h	Ref.
$Fe(CO)_5$	$THF/(CH_3)_3N$	23.8	110	5	9
$Ru_3(CO)_{12}$	$THF/(CH_3)_3N$	23.8	100	3300	9
$[Ru(bipy)_2(CO)Cl]^+$	H_2	19.4	150	600	75
$Os_3(CO)_{12}$	$THF/(CH_3)_3N$	23.8	180	270	9
$Rh_6(CO)_{16}$	$THF/(CH_3)_3N$	23.8	125	1700	9
$Ir_4(CO)_{12}$	$THF/(CH_3)_3N$	23.8	125	300	9
$[Pt_3(CO)_6]_2^-$	$THF/(CH_3)_3N$	23.8	125	700	9
$Rh_6(CO)_{16}$	$EtOCH_2CH_2OH/NH_2CH_2CH_2NH_2$	0.8	100	250	63
$Rh_6(CO)_{16}$	$EtOCH_2CH_2OH/NH_2(CH_2)_3NH_2$	0.8	100	76	63
$Rh_6(CO)_{16}$	$EtOCH_2CH_2OH/NH_2(CH_2)_4NH_2$	0.8	100	15	63

Table 5. AMINE-PROMOTED RUTHENIUM CATALYSIS OF THE WGSR

Catalyst	Solvent /Amine	Pressure CO (atm)	Temp. (°C)	Turnovers /10 h	Ref.
$Ru_3(CO)_{12}$	$Diglyme/(CH_3)_3N$	51	100	5740	52
$Ru_3(CO)_{12}$	$Diglyme/Et_3N$	51	100	860	52
$Ru_3(CO)_{12}$	$Diglyme/Bu_3N$	51	100	540	52
$Ru_3(CO)_{12}$	Diglyme/pyridine	51	100	300	52
$Ru_3(CO)_{12}$	$Diglyme/NH(CH_3)_2$	51	100	2200	52

Despite a decade of effort, several key questions concerning ruthenium carbonyl WGSR catalysis under base-promoted conditions remain to be clarified. These include

(1) Do mononuclear or dinuclear species participate to any extent in WGSR catalysis and are these species involved in the equilibria between the active trimer, $HRu_3(CO)_{11}^-$, and the inactive or less active $H_3Ru_4(CO)_{12}^-$?

(2) What species are responsible for H_2 elimination?

(3) Is the hydroxide-promoted ruthenium WGSR system analogous to the amine-promoted system?

Most recently, a new type of mononuclear/dinuclear ruthenium WGSR catalysis system was described by Shvo et al.[54] The system is based on the reaction of tetra-phenylcyclopentadienone (CPD) ruthenium tricarbonyl, (η-4 CPD)$Ru(CO)_3$, with OH^-. The mechanism, as shown in Scheme 6, involves the formation of several extremely unusual intermediates. In reaction (44), or just prior, the tetrahapto-CPD complex is transformed into a complex containing a pentahapto hydroxycyclopentadienyl ligand and a ruthenium hydride, $(HOCp)Ru(CO)_2H$, rather than the expected dihydride. The $(HOCp)Ru(CO)_2H$ complex can readily dimerize with loss of hydrogen to give a dimer, $(CO)_2Ru(CpO\text{-}\mu\text{-}H)(\mu\text{-}H)\text{-}(O\text{-}Cp)Ru(CO)_2$, whose x-ray structure indicates that it contains both a bridging hydride and a bridging proton. Reaction (45) represents an unusual form of reaction (31), wherein HX is the monomer $(HOCp)Ru(CO)_2H$. In addition, the unique structure of $(HOCp)Ru(CO)_2H$ suggests that the metallocarboxylic acid intermediate may also have unusual bonding interactions.

$$CPDRu(CO)_3 + OH^- \longrightarrow [CPDRu(CO)_2CO_2H]^-$$

$$[CPDRu(CO)_2CO_2H]^- \longrightarrow CPDRu(CO)_2H^-$$

$$CPDRu(CO)_2H^- + H_2O \longrightarrow CPDRu(CO)_2H_2 + OH^- \qquad (44)$$

$$2CPDRu(CO)_2H_2 \longrightarrow [CPDRu(CO)_2H]_2 + H_2 \qquad (45)$$

SCHEME 6

The dimer is air stable and represents a useful precursor for the WGSR catalyst system. However, its most important feature may be its apparent stability in the presence of H_2S.

Doi and Tamura have briefly described[55] the use of a totally aqueous phase ruthenium WGSR catalyst system, $RuCl_3/KOH/H_2O$, which is more active in the absence of an ethoxyethanol co-solvent than in its presence (see Table 3). Only limited kinetic studies were performed and no attempt was made to identify any intermediates.

Group 6 Metal Complexes

King et al.[49,56] were the first group of researchers to report the use of group 6 metal carbonyls [$Cr(CO)_6$, $Mo(CO)_6$, $W(CO)_6$] as catalyst precursors for catalysis of the WGSR in the presence of OH^-. Based on kinetic studies of WGSR catalyst solutions generated from these three carbonyl complexes, King et al. suggest the following general catalytic cycle:

$$CO + OH^- \longrightarrow HCO_2^-$$

$$M(CO)_6 \rightleftharpoons M(CO)_5 + CO$$

$$M(CO)_5 + HCO_2^- \longrightarrow M(CO)_5(O_2CH)^-$$

$$M(CO)_5(O_2CH)^- \longrightarrow HM(CO)_5^- + CO_2 \qquad (46)$$

$$HM(CO)_5^- + H_2O \longrightarrow H_2M(CO)_5 + OH^-$$

$$H_2M(CO)_5 \longrightarrow M(CO)_5 + H_2$$

SCHEME 7

This type of mechanism is supported by the results of Slegeir et al.,[57] who show that thermally and photochemically activated group 6 metal carbonyls can catalyze the decomposition of formates to H2 and CO2. Weiller et al.[58] have also examined the photoinitiated decomposition of formate in the presence of Cr(CO)6 and W(CO)6. Their

kinetic and mechanistic studies concur with the mechanism proposed by King et al. These studies, which are extremely detailed, lead to the conclusion that decarboxylation is the rate-determining step; it occurs with activation enthalpies of 26.0 and 24.8 kcal/mol for Cr and W, respectively.

A contrasting argument has been presented by Darensbourg and coworkers,[19,28] who find that the reaction that produces the anionic metal hydride and CO_2 is actually an equilibrium favoring the metalloformate (46) and thus is not a particularly useful intermediate. In addition, from kinetic studies of the reaction of $M(CO)_6$ with base, they find that

$$M(CO)_6 + OH^- \longrightarrow M(CO)_5CO_2H^-$$

$$M(CO)_5CO_2H^- \longrightarrow M(CO)_5H^- + CO_2$$

$$M(CO)_5H^- \longrightarrow M(CO)_5H^- + OH^-$$

$$M(CO)_5H_2 \longrightarrow M(CO)_5 + H_2$$

$$M(CO)_5 + CO \longrightarrow M(CO)_6$$

SCHEME 8

Because Weiller et al.[58] and Darensbourg et al.[19,28] performed their studies at much lower temperatures than King et al.,[49-50] it is not clear that their kinetic results are totally applicable to predicting the rate-determining step under King's conditions.

Klingler et al.[59] provide the first thermodynamic data concerning equilibria such as shown in reaction (46). They find that nBu_3SnH will react reversibly with CO_2 to give nBu_3SnO_2CH, reaction (47).

$$nBu_3SnH + CO_2 \rightleftharpoons nBu_3SnO_2CH \qquad (47)$$

Over the temperature range of 115°-175°C, they find that for the forward reaction (formate formation), $\Delta H = -18.3$ kcal/mol and $\Delta S = -20.2$ kcal/mol. Whether these thermodynamics are applicable to reaction (46) or related reactions remains to be seen.

Rhodium WGSR Catalyst Systems

Laine et al.[60,61] briefly explored the WGSR catalysis chemistry of $Rh_6(CO)_{16}$/KOH systems. Although the evidence is incomplete because of the extreme complexity of the cluster equilibria, a very simplified catalytic cycle can be written based on spectroscopically identified species and on the work of Chini et al:[62]

$$Rh_6(CO)_{16} + OH^- \longrightarrow HRh_6(CO)_{15}^- + CO_2$$

$$2HRh_6(CO)_{15}^- \longrightarrow H_2 + Rh_{12}(CO)_{30}^{2-}$$

$$Rh_{12}(CO)_{30}^{2-} + 2CO + 2H_2O \longrightarrow Rh_6(CO)_{16} + H_2 + 2OH^-$$

SCHEME 9

Kaneda et al.[63] studied $Rh_6(CO)_{16}$/amine WGSR catalyst systems. They found that diamines such as ethylene diamine considerably enhance the activity of the catalyst (see Table 5). They conclude that amine configuration plays a more important role in determining catalyst activity than amine basicity, which suggests that the amines function both as base and as ligands in the WGSR catalytic cycle.

Two drawbacks to using primary or secondary amines as cocatalysts are the well-known formamidation reaction (48) and urea synthesis reaction (49), both of which can lead to irreversible loss of amine:

$$R_2NH + CO \xrightarrow{\text{catalyst}} R_2NC(=O)H \qquad (48)$$

$$2RNH_2 + CO \xrightarrow{\text{catalyst}} RNH(C=O)HNR + H_2 \qquad (49)$$

Reaction (50), the transalkylation reaction,[53] can change the amine configuration considerably and may also diminish the effectiveness of WGSR catalyst systems that use primary or secondary amine promoters by disproportionating all the amine into tertiary amine species.

$$2R_2NH \xrightarrow{\text{catalyst}} R_3N + RNH_2 \qquad (50)$$

No detailed studies have been reported to date on the kinetics or mechanisms of the $Rh_6(CO)_{16}$/amine WGSR system, again emphasizing the need for research in the area of amine promoters.

Iridium WGSR Catalyst Systems

Iridium-catalyzed WGSR systems were described some time ago and detailed kinetic studies were reported by Vandenberg et al. in 1989[3]. Their observations lead them to propose the following catalytic cycle:

$$Ir_4(CO)_{12} + OH^- \longrightarrow HIr_4(CO)_{11}^- + CO_2$$

$$HIr_4(CO)_{11}^- + OH^- \longrightarrow [HIr_4(CO)_{11}(CO_2H)^{2-}]$$

$$[HIr_4(CO)_{11}(CO_2H)^{2-}] \longrightarrow H_2Ir_4(CO)_{11}^{2-} + CO_2$$

$$H_2Ir_4(CO)_{11}^{2-} + H_2O \longrightarrow H_3Ir_4(CO)_{10}^- + OH^-$$

$$H_3Ir_4(CO)_{10}^- + CO \longrightarrow HIr_4(CO)_{11}^- + H_2$$

SCHEME 10

At low CO pressures, an irreversible side reaction involving formation of the dimer [reaction (51)] is observed.

$$2HIr_4(CO)_{11}^- \longrightarrow H_2 + 2CO + Ir_8(CO)_{20}^{2-} \qquad (51)$$

The dimer exhibits only slight WGSR catalyst activity. The catalyst system was also found to be active for formate decomposition. Its formate decomposition activity is almost twice that of its WGSR activity under similar conditions. On the basis of this observation, Vandenberg et al.[31] suggest that a useful alternative to the catalytic cycle proposed in Scheme 10 would be a catalytic cycle based on formate decomposition analogous to that shown in Scheme 7. No evidence is presented that permits differentiation between the two possibilities.

The rate-limiting step in iridium cluster catalysis of the WGSR is hydroxide attack on $HIr_4(CO)_{11}^-$, followed by decarboxylation to $H_2Ir_4(CO)_{10}^{2-}$. The apparent activation energy for the overall catalytic process, determined for the temperature range of 90-130°C, is 10.7 kcal/mol.

Mixed-Metal Catalysis of the WGSR

Mixed-metal catalysis of the WGSR and the related Reppe reactions have been reported in the literature. One system, described by Ford et al.,[64] involves the use of iron/ruthenium mixtures to catalyze the WGSR. Two reports concern the use of iron/ruthenium or iron/rhodium mixture for the hydroformylation reaction.[65] As seen in Table 3, the use of mixtures of iron and ruthenium in place of the individual metals in conjunction with OH^- gives catalyst solutions that are more active than identical catalyst solutions made up of the individual metals.

At present, there is no firm evidence to provide a rationale for these observations. However, the two most reasonable explanations are that a mixed-metal cluster forms during the reaction and it either undergoes more facile reductive elimination of H_2 than the single metal catalyst intermediates or is more susceptible to OH^- attack. Knox et al.[66] report that the cluster $H_4FeRu_3(CO)_{12}$ loses H_2 more readily than the all-ruthenium analog. In the related Reppe hydroformylations, mixed-metal rate enhancement is observed where essentially no H_2 is produced, thus making the first conclusion unlikely. Gross and Ford[13] find that the order of reactivity for the iron triad clusters, for nucleophilic attack by methoxide, is $Fe_3(CO)_{12} > Ru_3(CO)_{12} > Os_3(CO)_{12}$. They propose that the iron cluster is more reactive than the ruthenium or osmium clusters, because it alone, of the three, contains bridging carbonyl groups. Iron may also cause the formation of bridging carbonyls in the mixed-metal cluster, making it more susceptible to nucleophilic attack by OH^-. This explanation is also reasonable for the iron/ruthenium Reppe hydroformylation catalysts.

A thorough study of mixed-metal catalysis of the WGSR was recently reported by Venäläinen et al.[67] They carefully studied the WGS activity of well characterized group VIII metal clusters with pyridine as the base. They present their data very nicely, as shown in Table 6, where they enter maximum observed activity for the metal mixtures. Under their conditions Rh compounds had the highest activity, but all the complexes had rather modest activity compared with other literature data (ruthenium cluster had TF < 1). The sulfur tolerance of rhodium- and cobalt-based catalysts is questionable. However, this study is a direct comparison that demonstrates that,under these reaction conditions,the cobalt rhodium cluster is 3 times the activity of a iron ruthenium cluster and 50 times the activity of a ruthenium cluster.

Table 6: Catalytic Activity of Group VIII Metal Carbonyl Precursors (cycles per day) (ref. 67)

	Fe	Ru	Os	Co	Rh	Ir
Fe	5	250	0	0	30	32
Ru		15	c	36	140	24[a]
Os			0	c	c	3[b]
Co				0	700	1
Rh					590	130
Ir						3

a. Activity of a mixture of $RuCl_3$ and $[Ir(CO)_3Cl_2]_2$ as a catalyst precursor.
b. Activity of a mixture of $Os_3(CO)_{12}$ and $[Ir(CO)_3Cl_2]_2$.
c. Not studied.

CATALYSIS OF THE WGSR UNDER ACIDIC OR NEUTRAL CONDITIONS

The first two examples of homogeneous catalysis of the WGSR using acidic media were reported in 1977. One WGSR system, described[10] and patented[68] by Eisenberg and Cheng, uses a rhodium catalyst in acetic acid/HI solution. The second system, reported by Zudin et al.[11] and essentially unnoticed in the literature, involves the use of palladium phosphine complexes in trifluoroacetic acid.

In continuing work on the rhodium system, Baker et al.[69] describe kinetic and mechanistic investigations that suggest the catalytic cycle shown in Scheme 11.

$$Rh(CO)_2I_3^- + HI \rightleftharpoons H_2 + Rh(CO)_2I_4^-$$

$$Rh(CO)_2I_4^- + CO \rightleftharpoons I^- + Rh(CO)_3I_3$$

$$Rh(CO)_3I_3 + H_2O \rightleftharpoons H^+ + Rh(CO)_2I_3(CO_2H)^-$$

$$Rh(CO)_2I_3(CO_2H)^- \longrightarrow HI + Rh(CO)_2I_2^- + CO_2$$

$$Rh(CO)_2I_2^- + HI \rightleftharpoons HRh(CO)_2I_3^-$$

or

$$Rh(CO)_2I_3(CO_2H)^- \longrightarrow HRh(CO)_2I_3^- + CO_2$$

and

$$Rh(CO)_2I_4^- + I^- \rightleftharpoons CO + Rh(CO)I_5^-$$

SCHEME 11

Baker et al. have spectroscopically identified the species $Rh(CO)_2I_2^-$, $Rh(CO)I_5^-$, $Rh(CO)I_4^-$ in solution and have isolated and characterized $Rh(CO)_2I_2^-$. An Arrhenius plot of the WGSR catalysis over the range of 55°-100°C reveals unusual behavior, giving an Ea of 25.8 kcal/mol between 55°-60°C and an Ea of 9.3 kcal/mol above this range. The authors argue that there is a change in the rate-limiting step at higher temperatures. Furthermore, they propose that at low temperatures the rate-limiting step is oxidation of Rh(I) by HI to Rh(III), and at high temperatures the rate-limiting step is reduction of a Rh(III) carbonyl species with concomitant release of CO_2.

These observations are similar to, but not completely in accord with, the work of Singleton and Forster, who studied the same system but under more forcing conditions.[70,71] The major difference appears to be that, at higher temperatures and pressures, WGSR is nearly independent of CO pressure at high acidity, but is inversely affected by changes in CO pressure at low acidities. These observations are the opposite of those of Cheng and Eisenberg, whose work was performed at subatmospheric pressures.

More recently, Marnot et al.[72,73] identified another rhodium WGSR catalyst that operates under acidic conditions. These workers report that rhodium and iridium 2,2'-bipyridine (bipy) or related ligand complexes such as $Rh(bipy)_2(H_2O)^{3+}$, $Rh(L)_2(H_2O)^{3+}$,

and $Ir(L)_2(H_2O)^{3+}$, where L = 4,7-diphenyl-1,10-phenanthroline disodium sulfonate (Phen-S) or L = 2,9-dimethyl-4,7-diphenyl-1,10-phenanthroline disodium sulfonate (2,9-dmphen-S), are active WGSR catalysts under acidic conditions. Aside from the catalyst activities listed in Table 7, no mechanistic work has as yet been reported. However, the authors do suggest that in the case of iridium, the much higher activity of the 2,9-dimethylphen complexes as compared with the simple phen complexes can be ascribed to steric hindrance between the methyl groups that prevents the formation of stable square planar, inactive bis(dimethylphen) complexes.

In a somewhat related study, Alessio et al.[74] examined the WGSR catalyst activity of mixtures of $Ru_3(CO)_{12}$, $Os_3(CO)_{12}$, and $Ir_4(CO)_{12}$ with the same types of 2,2'-bipyridyl (bipy) and phenanthroline (phen) ligands as Marnot et al.; however, they examined these systems only in the presence of nitrobenzene. Their objective was to examine the activity of these systems for the catalytic reduction of nitrobenzene to aniline. In these studies, only the ruthenium system was active, with the phen/Ru system exhibiting greater activity than the bipy/Ru system under the conditions studied. Unfortunately, no attempts appear to have been made to test these systems for WGSR activity, although they have been studied under basic conditions.[75]

Mahajan et al.[76] have reported studies of polypyridine rhodium complexes that provide some mechanistic explanations about the WGSR catalysis systems originally described by Marnot. In their studies of rhodium WGSR catalysis in the presence of phen, bipy, pyrazine, and 4,4'dimethyl-bipy, they were able to obtain spectroscopic and kinetic evidence suggesting that the active catalyst species under acidic conditions is likely to be $Rh(bipy)_2(CO)H^{2+}$. Scheme 12 is suggested as a reasonable catalytic cycle.

$$Rh(bipy)_2(CO)H^{2+} + H_2O \longrightarrow [Rh(bipy)_2(CO_2H)H^{2+}] + H^+$$

$$[Rh(bipy)_2(CO_2H)H^+] \longrightarrow Rh(bipy)_2H_2^+ + CO_2$$

$$Rh(bipy)_2(CO)H_2^+ \longrightarrow Rh(bipy)_2^+ + H_2$$

$$Rh(bipy)_2^+ + CO \longrightarrow Rh(bipy)_2(CO)^+$$

$$Rh(bipy)_2(CO)^+ + H^+ \longrightarrow Rh(bipy)_2(CO)H^{2+}$$

SCHEME 12

The system illustrated in Scheme 12 shows optimal activity at pH 3, leading the authors to suggest that metallocarboxylic acid formation or decarboxylation is the slow step in the reaction. They also conclude that the active catalyst species is a Rh^{3+} complex formed in the protonation step (see Scheme 12). Mahajan et al. also find that, under CO, significant equilibria exist between the $Rh(bipy)_2^+$ species and free bipy. Interestingly, formation of free bipy is enhanced by increasing the pH, contrary to what might be expected. These results are extremely pertinent to those of Marnot et al., because the latter authors find that the ligand-to-metal ratios in their systems strongly affect the overall WGSR catalyst activities and that different ratios are preferable for optimal rhodium activity (2:1) and optimal iridium activity (1:1).

In the platinum metals group, both palladium and platinum complexes have been shown to be active WGSR catalysts in the presence of acid cocatalysts. Likholobov et al.[77] have followed up on the original report by Zudin et al.[11] and propose the catalytic cycle shown in Scheme 13 for Ph_3P-complexed palladium WGSR catalysis system run in 20% aqueous trifluoroacetic acid.

$$P_2PdX_2 + CO \rightleftharpoons [P_2Pd(X)CO]^+ + X^-$$

$$[P_2Pd(X)CO]^+ + H_2O \rightleftharpoons [P_2Pd(H_2O)CO]^{2+} + X^-$$

$$[P_2Pd(H_2O)CO]^{2+} + H_2O \rightleftharpoons [P_2Pd(OH)CO]^+ + H_3O^+$$

$$[P_2Pd(OH)CO]^+ + X^- \longrightarrow P_2Pd(CO_2H)X$$

$$P_2Pd(CO_2H)X \longrightarrow P_2PdHX + CO_2$$

$$P_2PdHX + HX \longrightarrow P_2PdX_2 + H_2$$

$$P = Ph_3P,\ HX = CF_3CO_2H$$

SCHEME 13

In view of the work of Cariati et al.,[42b] reaction (35), the mechanism proposed in Scheme 13 appears quite reasonable.

More recently, Giannoccaro et al.[78] have reported the existence of nickel-based WGSR systems similar to those of Zudhin et al. The Giannoccaro work demonstrates that

NiX_2P_2 complexes, where X = Cl or Br and P = basic phosphines such as PR_3 (R = Me, Et, Bu, iPr), will catalyze the WGSR under 1 atm of CO at 90°-160°C in the presence of up to five equivalents of acid (see Table 7). The WGSR mechanism proposed is essentially that of Zudin et al., although in the nickel system it is possible to observe and/or isolate species such as $(CO)_2NiP_2$ and $(CO)X_2NiP_2$, which are not stable in the palladium system. The Giannoccaro systems are not very stable, giving metal and or inactive systems after only a few days of activity.

In addition to their studies on rhodium WGSR catalysis in acid media, Cheng and Eisenberg also report[79] that mixtures of platinum chloride and tin chloride are active WGSR catalysts in an acetic acid/HCl solvent system. They report that a spectroscopic analysis of the active catalyst solution shows the presence of both $PtCl(CO)(SnCl_3)_2^-$ and $PtCl_2(CO)(SnCl_3)^-$. Preliminary kinetic and mechanistic studies allow them to suggest the catalytic cycles shown in Scheme 14.

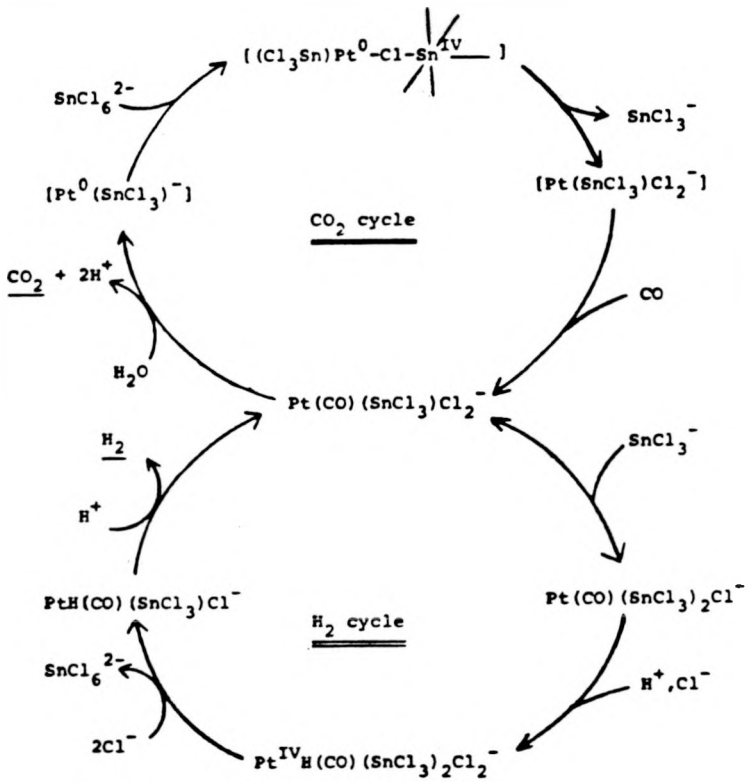

SCHEME 14

These researchers conclude that the Sn(II)/Sn(IV) redox couple is actively involved in the observed reaction chemistry. The H_2-forming catalytic cycle results in the oxidation of Sn(II) to Sn(IV), with coproduction of H_2, and CO is oxidized to CO_2 concurrent with the reduction of Sn(IV) to Sn(II).

Ford and coworkers[80,81] have reported that ruthenium carbonyl will also catalyze the WGSR under acidic conditions. Thus, mixtures of either $Ru_3(CO)_{12}$ or $H_4Ru_4(CO)_{12}$ in a solvent system of H_2SO_4 in diglyme or ethoxyethanol give the same active WGSR catalyst system that functions at 100°C, as shown in Table 7. The system is first-order-dependent on both ruthenium concentration and CO pressure (below 1 atm), but shows little or no dependence on acidity or water concentration over the ranges studied. Above 1 atmosphere of CO, there was a considerable decrease in reactivity that was at least partially due to the enhanced formation of $Ru_3(CO)_{12}$, which sublimed out of the reaction solution. The apparent activation energy for WGSR catalysis was 14 kcal/mol over the temperature range of 90°-140°C. From kinetic and spectroscopic studies, Yarrow et al.[81] concluded that the reduced anionic species [e.g., $HRu_2(CO)_8^-$], previously proposed as the likely participants in the WGSR catalytic cycle, do not form. They now propose a catalytic cycle based on solvent-substituted ruthenium dimers, as seen in Scheme 15:

$$HRu_2(CO)_{9-x}(OR_2)_x^+ + CO \longrightarrow HRu_2(CO)_{10-x}(OR_2)_{x-1}^+ + OR_2$$

$$HRu_2(CO)_{10-x}(OR_2)_{x-1}^+ + H_2O \longrightarrow HRu_2(CO)_{9-x}(CO_2H)(OR_2)_{x-1} + H^+$$

$$HRu_2(CO)_{9-x}(CO_2H)(OR_2)_{x-1} \longrightarrow H_2Ru_2(CO)_{9-x}(OR_2)_{x-1} + CO_2$$

$$H_2Ru_2(CO)_{9-x}(OR_2)_{x-1} + OR_2 \longrightarrow Ru_2(CO)_{9-x}(OR_2)_x + H_2$$

$$Ru_2(CO)_{9-x}(OR_2)_x + H^+ \longrightarrow HRu_2(CO)_{9-x}(OR_2)_x^+$$

SCHEME 15

Yarrow et al.[81] examined the possibility of enhancing the activity of the ruthenium system under acidic conditions through the addition of $Fe(CO)_5$, which significantly promotes ruthenium WGSR catalysis in alkaline solution. Unfortunately, no effect was observed. In addition, they also find that $Ir_4(CO)_{12}$, which is active in alkaline solutions, shows no WGSR activity under acidic conditions.

Kaspar et al.[82] describe an active WGSR system based on rhodium/phosphine catalyst species that function in dioxane/water mixtures, both in base and in acid. The acid-promoted catalyst systems are more active than the base-promoted systems. The data for the catalyst deriving from the precursor complex $Rh(COD)(PPh_3S)_2^-$, where PPH_3S^- is

meta-monosulfonated triphenylphosphine, are listed in Table 7. The authors are hesitant to propose a mechanism for their observations because of the unusual results and the limited amount of data. However, it seems reasonable to suggest that the electron-rich metal might promote reactions such as suggested above, in which CO binding is followed by protonation of the complex and subsequent nucleophilic attack of water on the protonated complex to give a metallocarboxylic acid, and so forth.

Before 1987, only three WGSR catalyst systems had been described for which it was not necessary to activate and maintain the catalytic reactivity of the system through addition of either base or acid. One reaction system uses platinum phosphine catalysts, and the other two systems use rhodium phosphine catalysts. The one platinum system and one of the rhodium systems were described by Yoshida et al.[24,33] These investigators report catalyst systems that function by H_2O activation, in sharp contrast to the systems described above, which all apparently function by CO activation.

Yoshida et al.[24] reported in 1978 that platinum phosphine complexes of the type PtL_3, where L = $P(iPr)_3$ or PEt_3, could be used to catalyze the WGSR under mild conditions in a number of solvents. They proposed the catalytic cycle shown in Scheme 16 to account for their observations.

$$PtL_3 \rightleftharpoons PtL_2 + L$$

$$PtL_2 + H_2O \rightleftharpoons PtH(OH)L_2$$

$$PtH(OH)L_2 + S \rightleftharpoons [PtH(S)L_2]OH$$

$$[PtH(S)L_2]OH + CO \rightleftharpoons [PtH(CO)L_2]OH + S$$

$$PtH(CO)L_2]OH \rightleftharpoons [PtH(CO_2H)L_2]$$

$$[PtH(CO_2H)L_2] \rightleftharpoons PtH_2L_2 + CO_2$$

$$PtH_2L_2 + L \rightleftharpoons PtL_3 + H_2$$

SCHEME 16

Table 7. CATALYSIS OF THE WGSR UNDER ACID OR NEUTRAL CONDITIONS

Catalyst	Solvent /amine	CO Pressure (atm)	Temp. (°C)	Turnovers /24 h	Ref.
$[Rh(CO)_2Cl]_2$	HI/HOAc	0.53	100	34	10
$RhCl_{3.3}\cdot H_2O$/2.2,9-dmphen-S	H_2O	1.0	100	550	72
$IrCl_{3.3}\cdot H_2O$/2.2,9-dmphen-S	H_2O	1.0	100	225	72
$IrCl_{3.3}\cdot H_2O$/bipy-S	H_2O	1.0	100	9.6	72
$Pd(PPh_3)_4$	CF_3CO_2H	1.0	70	60	77
$NiCl_2(PMe_3)_2$	EtOH	1.0	130	0.016	78
$NiCl_2(PMe_3)_2$	EtOH	1.0	160	0.03	78
$K_2PrCl_4/SnCl_4\cdot H_2O$	HCl/HOAc	0.53	80	25	79
$Ru_3(CO)_{12}$	H_2SO_4/diglyme	1.0	100	60	81
$Rh(COD)PPh_3S$	Dioxane/H_2O				
	pH = 11	30	155	168	82
	pH = 8	30	155	144	82
	pH = 6	30	155	84	82
	pH = 4	30	155	432	82
	pH = 2	30	155	3050	82
$Pt[P(iPr)_3]_3$	Acetone	19.3	100	125	24
$RhH[P(iPr)_3]_3$	Acetone	19.3	100	672	33
$RhH[P(iPr)_3]_3$	Pyridine	19.3	100	792	33
$Rh_2(H)(CO)_3(DPPM)^+$	PrOH	1.0	90	60	84
$Rh_2(\mu\text{-}CO)(CO)_2(\mu\text{-}DPM)_2$		0.66	90	14	85
$Rh_2(\mu\text{-}H)(\mu\text{-}DPM)_2]PF_6$		3.0	100	90	86

Complexes such as trans-$PtH(CO_2K)L_2$, trans-$PtH(CO_2CH_3)L_2$, and trans-PtH_2L_2 were prepared as examples of the proposed intermediate, and the latter complex was independently shown to catalyze the WGSR.

In the neutral rhodium system[33] the complex $RhHL_3$, where L = $P(i\text{-}Pr)_3$ or $P(c\text{-}C_6H_{11})_3$, was found to be an active WGSR catalyst in either acetone, THF, or pyridine, with the pyridine (py)-solvated reaction having the higher catalyst activity. The following reaction sequence is proposed for the catalytic cycle:

$$RhHL_3 + H_2O + py \rightleftharpoons [RhH_2(py)_2L_2]OH$$

$$[RhH_2(py)_2L_2]OH + CO \rightleftharpoons [Rh(CO)(py)_2L_2]OH + H_2$$

$$[R(CO)(py)_2L_2]OH + CO \rightleftharpoons [Rh(CO)_2(py)L_2]OH + py$$

$$[Rh(CO)_2(py)L_2]OH \longrightarrow [Rh(CO)(CO_2H)(py)L_2]$$

$$Rh(CO)(CO_2H)(py)_2L_2 + CO \longrightarrow RhH(CO)_2L_2 + CO_2 + py$$

$$RhH(CO)_2L_2 + H_2O \rightleftharpoons [RhH_2(CO)L_2]OH$$

$$[RhH_2(CO)L_2]OH + py \rightleftharpoons [Rh(CO)(py)L_2]OH + H_2$$

SCHEME 17

The complexes trans-$[Rh(CO)(py)L_2]^+$ and $[RhH_2(py)_2L_2]OH$ can be isolated when pyridine is used as solvent. When acetone is the solvent, $RhH(CO)_2L_2$ can be isolated from the reaction solutions, as can the complex $Rh_2(CO)_4L_2$. Most of these complexes were shown spectroscopically or in separate reaction studies to react as shown in Scheme 17.

A recent set of papers describe the use of DPM (bis-diphenylphosphinomethane) ligands to form cluster complexes of rhodium,[83,84] iridium,[85] and platinum[86,87] that all promote the WGSR under neutral conditions and do not require the addition of acid or base. The earliest report was that of Kubiak and Eisenberg,[83] who mentioned that the complex $[Rh_2(\mu\text{-}H)(\mu\text{-}CO)(CO)_2(DPM)_2]^+$ was an active WGSR catalyst under neutral conditions. In a later paper,[84] they report that, in the presence of one equivalent of toluene

sulfonic acid and two equivalents of a salt (e.g., LiX, X = Cl, Br), the catalyst system was most active at near neutral pH. The presence of carboxylate salts, including formate salts, diminished catalyst activity. Additionally, the catalyst system deactivated over time, under all conditions studied. The former observation suggests that formates do not participate in the catalytic cycle. The authors discuss a catalytic cycle based on formate decomposition but their data, specifically with regard to the inhibitory effect of formate, make this cycle suspect; however, their discussions do suggest another type of catalytic cycle akin to the one proposed later by Sutherland and Cowie[85] (Scheme 18).

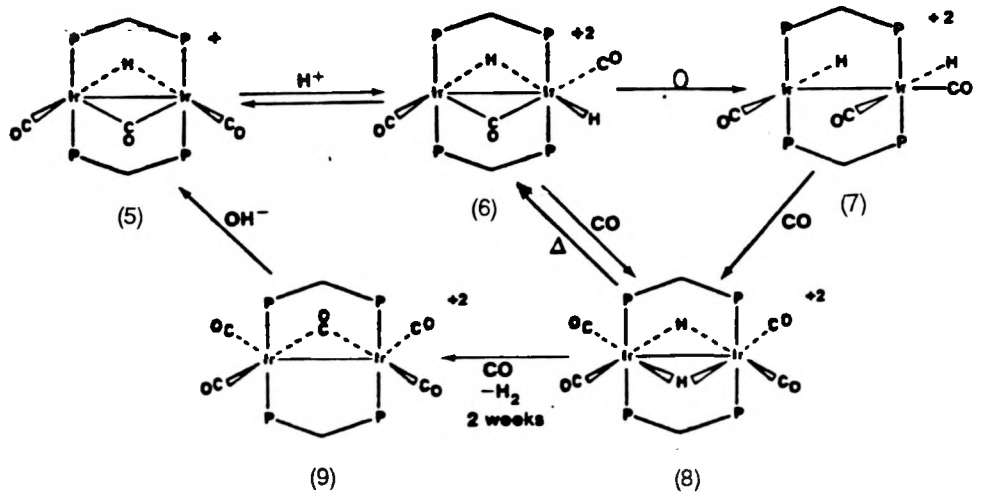

SCHEME 18

Most recently, Sutherland and Cowie[85] have extended the work of Kubiak and Eisenberg through studies of both the original rhodium system and its iridium analog. Their work was initially based on the hypothesis that a bridging hydroxide would be a likely intermediate in the catalytic cycle; however, they disprove this hypothesis. Sutherland and Cowie suggest a potential catalytic cycle based on their iridium studies (Scheme 18) that could be applicable to the rhodium system; however, the step resulting in loss of H_2 from the iridium analog requires two weeks!

Puddephatt and coworkers[86,87] report that $[Pt_2H_2(\mu\text{-}H)(\mu\text{-}DPM)_2]PF_6$ is a precursor to a quite active WGSR catalyst (see Table 6) whose activity is strongly dependent on CO pressure. They suggest the catalytic cycle shown in Scheme 19.

$$Pt_2H_2(\mu\text{-DPM})_2^+ + CO \longrightarrow Pt_2HCO(\mu\text{-DPM})_2^+ + H_2$$

$$Pt_2HCO(\mu\text{-DPM})_2^+ + OH^- \longrightarrow Pt_2H(CO_2H)(\mu\text{-DPM})_2$$

$$Pt_2(CO_2H)(\mu\text{-DPM})_2 + H^+ \longrightarrow Pt_2H_2(\mu\text{-H})(\mu\text{-DPM})_2 + CO_2$$

Scheme 19

The proposed cycle in Scheme 19 raises some questions. For example, if the work is conducted in a neutral solution, then what is the source of hydroxide? Sutherland and Cowie's work suggests that an intermediate bridging hydroxide might form upon reaction of the starting complex with water. If not, then it is known that carbonyls bound to positively charged metal complexes can react directly with water to form metallocarboxylic acids. These possible alternatives to the Scheme 19 cycle may have been overlooked.

WGSR Systems in the Presence of Sulfur Species

In the Introduction, the need for LT sulfur-tolerant WGSR catalysts was emphasized. Very little is currently known about the H_2S tolerance for any of WGSR systems currently described in the literature. King et al.[88] have demonstrated that, with the exception of iron, all the group 8 metal catalysts listed in Table 8 are active catalysts for the WGSR when Na_2S is substituted for OH^- as the base. Although the rates are low, this important contribution clearly demonstrates the considerable potential available for the use of homogeneous catalysts for industrially important processes.

Darensbourg et al.[89] briefly studied the reactions of SH^- with $Mn(CO)_6^+$, reaction (52), and with the group 6 metal carbonyls, reaction (53).

$$Mn(CO)_6^+ + SH^- \longrightarrow HMn(CO)_5 + CO_2 \qquad (52)$$

$$M(CO)_6 + SH^- \longrightarrow M(CO)_5SH^- + CO \qquad (53)$$

$$M = Cr, Mo, W$$

Table 8. SULFIDE-PROMOTED CATALYSIS OF THE WGSR

Catalyst	Solvent /Amine	CO Pressure (atm)	Temp. (°C)	Turnovers /24 h	Ref.
$Fe_3(CO)_5$	MeOH	27.2	140	0	67
$Ru_3(CO)_{12}$	MeOH	27.2	160	550	67
$Os_3(CO)_{12}$	MeOH	27.2	160	200	67
$Cr(CO)_6$	MeOH	27.2	160	60	67
$Mo(CO)_6$	MeOH	27.2	160	130	67
$W(CO)_6$	MeOH	27.2	160	180	67

Although $Mn(CO)_6^+$ does react as expected to give COS and a metal hydride, presumably via a metallothiocarboxylic acid, they were unable to observe a similar reaction with the group 6 metal carbonyls. However, their studies do suggest that a metallothiocarboxylic acid intermediate forms during reaction (53). These results could be extremely valuable in developing an understanding of how group 6 metal WGSR catalysts will function in the presence of SH^- generated from H_2 in an OH^--promoted system. Furthermore, it suggests that in the original studies of King et al. it may have been necessary for the added Na_2S to react with water to generate OH^- before WGSR catalysis could proceed. Based on the directives outlined in the Introduction concerning the need for tolerant WGSR catalysts, it seems reasonable that these catalyst systems require further study.

Ford[12] briefly mentions that the iron-ruthenium mixed-metal system rapidly loses iron upon exposure to H_2S; however, extensive studies of the system have yet to be performed to establish whether poisoning occurs under industrial conditions.

EXPERIMENTAL RESULTS

BATCH REACTOR

Catalyst Survey

We have surveyed some transition metal catalysts known to be active for the WGSR. The catalysts selected for testing and the conditions for the reaction are given in Table 9.

One of the most active catalysts for the WGSR under basic conditions has been $Ru_3(CO)_{12}$. Both hydroxyl and amine bases are effective promoters for this reaction. As expected, Group VI metal carbonyls were also active for the WGSR under these conditions. $Mo(CO)_6$ gave the faster rate versus. $Cr(CO)_6$. $Mo(CO)_6$ also showed a significant temperature dependence; the rate increased by a factor of 3 when the temperature was increased from 180° to 200°C.

Ruthenium and rhodium complexes containing bidentate nitrogen ligands have also been reported to catalyze the WGSR. We tested selected bipyridine and phenanthroline derivatives in triethylene glycol using K_2CO_3 as the base promoter. All complexes were prepared *in-situ* under the reaction conditions. Our results are listed in Table 10. The maximum TFs (turnover frequencies) observed for the $Ru_3(CO)_{12}$/bipyridine complexes were 5.9 (180°C) and 7.7 (200°C with NaSH added) at a metal-to-ligand ratio of 1:2. The rate was only moderately dependent on the ligand concentration.

Table 9. SELECTED HOMOGENEOUS CATALYST SYSTEMS FOR WGSR[a]

Number	System	TF
1	$Cr(CO)_6$/alcohol base	12
2	$Mo(CO)_6$/alcohol	28
3	$W(CO)_6$/alcohol base	4.2
4	$Ru_3(CO)_{12}$/alcohol/hydroxide	4.2
5	Ru/amine	86
6	$Fe(CO)_5/Ru(O)_{12}$/amine	43
7	Sulfonated rhodium/phenanthroline	5.9
8	Ruthenium/phenanthroline	3.3
9	Cobalt/phenanthroline	7
10	Meta-monosulfonated triphenyl phosphine/Rh	< 1

a Pressure, 25 atm; temperature, 450 K; solvent, diethyl glycol (or other high boiling solvent); feedstock, O_2-blown coal gas; feedstock sulfur, 1000 ppm H_2S; and duration, 20 h.

[b]TF = turnover frequency, i.e., mmoles H_2/mmole catalyst/hour.

Table 10. CATALYST SURVEY RESULTS

Catalyst[a]	Metal/Ligand	Temp. (°C)	TF w/NaSH	TF w/oNaSH
$Ru_3(CO)_{12}$	bipy (1:1)	180	4.4	4.9
		200	7.8	8.0
	bipy (1:2)	180	5.9	5.5
		200	7.7	8.2
		180	4.2	4.0
		200	6.3	7.8
	phen (1:)[b]	180	3.0	6.0
	LiI (1:)	180	4.5	3.2
		200	--	5.1
	LiI (1:5)	180	4.7	3.9
	1:1:1 LiI:bipyridine	180	3.8	3.9
	Tertiary amine[c]	180	0.9	1.1
		200	1.4	1.7
$Rh_6(CO)_{16}$	--	180	1.8	1.6
		200	2.2	2.6
	bipy (1:1)	180	1.8	1.8
		200	5.3	5.5
$RhCl_3 \cdot 3H_2O$	2,9Dimethphen-S (1:2)[b]	200	3.3	--
$Ru_3(CO)_{12}$ $Fe_3(CO)_{12}$(1:1)	--	180	7.8	5.1
		200	3.9	7.1
$Rh_6(CO)_{16}$ 1:2 $Fe_3(CO)_{12}$	--	180	5.4	--
		200	7.7	--
$Fe_3(CO)_{12}$	--	180	deactivated	1.6
	--	200	deactivated	1.6
$Mo(CO)_6$	--	180	3.9	4.3
	--	200	14	15.4
$Cr(CO)_6$	--	180	4.5	4.7
	--	200	5.9	6.5

TF = turnover frequency = mmoles H_2/mmole catalyst/hour.

[a]0.1 mmol catalyst, 0.262 mL (13.9 mmol) H_2O, 1 mg (0.018 mmol) NaSH, 0.15 gr (1.08 mmol) K_2CO_3, triethylene glycol to 15 mL total volume. [b]1.0 mL (55.6 mmol) H_2O. [c]Tertiary amine = N-Methylpiperidine at 180°C or N,N,N',N'-1,6-hexanediamine at 200°C.

At 180°C, the 1:1 ruthenium/bipyridine complex (TF=4.4) was less active than the 1:2 complex. This rate difference was not observed at 200°C.

Rhodium carbonyl was less active than ruthenium under these conditions. The rates for the rhodium-catalyzed reaction were less than 50% of the rates for ruthenium with the bipyridine ligand.

The rhodium/bipyridine systems were much more temperature-dependent than the ruthenium systems. Raising the temperature 20°C (from 180 to 200°C) increased the rate approximately 80% for $Ru_3(CO)_{12}$/bipyridine (1:1), but approximately 200% for $Rh_6(CO)_{16}$/bipyridine (1:1). Both of these metal complexes were tolerant to sulfur present at approximately 1000 ppm; in certain cases, the reaction was actually faster with added NaSH. However, these complexes show only a small improvement in rate over complexes without the added bidentate ligand(s).

We examined the effects of LiI on the $Ru_3(CO)_{12}$ catalyst system because LiI is known to promote other Ru-catalyzed CO reactions. In this case, the presence of LiI actually inhibited WGSR catalysis.

Reports have been published in which mixed metal catalysts were more active for the WGSR than the individual metal catalysts (see Background section: Mixed-Metal Catalysis of the WGSR). Table 10 lists our results with the $Fe_3(CO)_{12}/Ru_3(CO)_{12}$ and $Fe_3(CO)_{12}/Rh_6(CO)_{16}$ catalyst systems. We also tested a $Ru_3(CO)_{12}/Fe(CO)_5$ catalyst mixture in a 1:3 and 0.5:3 ratio (0.4 mmole catalyst total) for the reaction under optimum conditions for a ruthenium/amine catalyst system (see below: 360 psi, 200°C, 4.6 mmol hexanediamine, 55.6 mmol H_2O, and 1 mg (0.018 mmol) NaSH in triglyme).

The initial rates (mmoles H_2/mmoles catalyst/h) were much lower (6.1 and 5.0, respectively) than expected. However, if the rate (TF) is calculated based only on the amount of $Ru_3(CO)_{12}$ present (24.2 and 20.0), then there is good agreement with the rate of the ruthenium catalyst alone (TF = 23.6). $Fe(CO)_5$ therefore does not appreciably enhance the WGSR activity of Ru under these conditions.

Solvent Effect

Rates were compared for a ruthenium/amine system in the solvents triethylene glycol and triglyme. Triglyme was used in an effort to improve the reaction rates by minimizing the possible side reactions of an alcoholic solvent with CO/catalyst to produce formates.[90]

$$ROH + CO \xrightarrow[Ru_3(CO)_{12}]{H_2,\ 150°C} HCO_2R$$

As mentioned previously, amines are reported to be good promoters for the WGSR. We conducted several trials with N-methylpiperidine (b.p. 106°-107°C). At 180°C, with 0.97 M (14.6 mmole) H_2O and 0.27 M (4.11 mmole) of N-methylpiperidine, the initial rate was 7.6 TF in triglyme versus 1.7 TF in triethylene glycol. Holding the water constant at 0.970 M and varying the amine concentration, we obtained a maximum TF of 17.5 (200°C) at an amine concentration of 1.37 M (20.6 mmole) in triglyme. The reaction times were approximately 10-15 h; and 5.1-8.5 mmole H_2 were produced in these runs. The 95% conversion of CO to H_2, predicted from WGSR equilibrium gas-phase calculations, was not reached before the reactions stopped, indicating that other factors limit the long-term activity of this system.

The Group VI metals showed no activity in triglyme with N,N,N',N',tetramethyl-1,6-hexanediamine. We ascribe this behavior to insolubility and/or decomposition of the catalysts because a grey insoluble residue was observed after each attempted reaction.

Effect of Base

We varied both the base and water concentrations to determine their effect on the initial rate and hydrogen production for ruthenium and molybdenum carbonyl catalyst systems.

We explored the activity of $Ru_3(CO)_{12}$ using N,N,N',N'tetramethyl-1,6-hexanediamine as base in the nonreactive solvent triglyme. As shown in Table 11 for 3.70 M (55.6 mmole) water, the rate of the ruthenium-catalyzed WGSR increased with increasing amine concentration: up to a TF of 52.1 (200 °C) for 2.15 M (32.2 mmole) or up to a TF of 53.6 (180°C) for 4.36 M (65.5 mmole) amine. When the amine concentration was varied from 0.312 to 4.36 M at 180°C, the rate approx. quadrupled, from 13.7 to 53.6. Concurrently, the time until we reach equilibrium in our system decreased with an increase in the amine: 9.3 h at 0.312 M to 4.9 h at 4.14 M at 200°C.

The maximum initial rate (TF) we have observed for the ruthenium system is 56.5, which occurred at 4.14 M (62.1 mmole) amine with 5.56 M (83.3 mmole) H_2O (180°C).

Table 11. WGSR RATE VERSUS AMINE CONCENTRATION

Water Conc. M (mmol)[a]	Amine Conc. M (mmol)	Temp. (°C)	TF	Time (h)	(mmol) H_2 Produced
0.97 (14.6)	0.31 (4.6)	180	11.3	10.0	6.3
0.97 (14.6)	0.61 (9.2)	180	12.3	7.6	6.0
3.7 (55.6)	0.31 (4.6)	180	13.7	10.5	10.4
3.7 (55.6)	0.31 (4.6)	200	23.6	9.6	12.2
3.7 (55.6)	0.61 (9.2)	200	27.1	8.5	11.1
3.7 (55.6)	0.92 (13.8)	200	33.0	6.3	(5.8)
3.7 (55.6)	2.2 (32.2)	200	52.1	5.2	13.9
3.7 (55.6)	3.1 (46.0)	180	51.5	4.9	12.9
3.7 (55.6)	3.1 (46.0)	200	51.6	5.2	14.0
3.7 (55.6)	4.4 (65.5)	180	53.6	4.2	13.2
11.1 (166.8)	3.7 (55.2)	180	52.8	4.9	13.5
22.2 (333.6)	2.8 (41.4)	180	48.5	5.1	12.9

[a]$Ru_3(CO)_{12}$ (0.1 mmol), N,N,N,N-1-6-hexanediamine, triglyme added to a total volume of 15 mL, 1 mg (0.018 mmol) NaSH, 360 psi.

This high rate was derived in a reaction containing only amine and water (i.e., no other organic solvent) and is effectively the upper limit for basicity with this amine.

At this concentration, increasing the temperature 20°C actually decreased the rate to 48.0. A possible explanation for the rate reduction was that CO was being consumed in a side reaction that competed with the WGSR more successfully at higher temperature. Mass spectral analysis of the reaction solution, however, did not indicate the presence of MeOH, MeOMe, or $MeCO_2H$, products that would be expected from the reduction of CO.

Since the rate of the WGSR for $Ru_3(CO)_{12}$ varied with amine concentration, we decided to look at the effect of increasing the concentration of K_2CO_3 with the $Mo(CO)_6$ system. The conditions we employed were 14 mL triethylene glycol, 3.70 M (55.6 mmole) H_2O, 200°C. The rate increased from 15.4 at 0.0724 M (1.08 mmole) K_2CO_3 to a maximum at 0.362M (5.42 mmole) (TF = 26.0) but then decreased to a TF of 17.5 at 0.724 M (10.8 mmole). This maximum rate of 26.0 for $Mo(CO)_6$ under these conditions is comparable to the rate of 29.3 for $Ru_3(CO)_{12}$ under similar conditions (55.6 mmole H_2O, 4.6 mmole diamine, 200°C). The rate decrease upon adding more carbonate may have occurred because the triethylene glycol became saturated before dissolution of all the K_2CO_3.

Potassium carbonate has itself been reported to be a catalyst for the WGSR (see, for example ref. 91). Noted that, with 0.724 M K_2CO_3 but no metal species present, the TF (for 3.70 M H_2O) was $<<1$ at 200°C.

Other alkali bases were also compared with the activity of the potassium carbonate. Potassium hydroxide at low concentrations (0.072 M) demonstrated very high activity relative to potassium carbonate at identical conditions (TF = 41.8 versus 10.4). However, at higher concentrations the advantage disappears (TF = 23.5 KOH versus TF = 28.0 K_2CO_3 at 0.493 M). Potassium formate was also tested at the high concentration where it demonstrates much lower activity (TF = 8.8 at 0.493 M).

Water Concentration

The rate of the WGSR for the $Ru_3(CO)_{12}$ system in triglyme was also found to depend on the amount of water present in the reactor (Table 12). The optimum water concentration proved to be 5.56 M (83.3 mmole) for several amine concentrations (Figure 4).

Table 12. RU-CATALYZED RATE VERSUS WATER CONCENTRATION

Water Conc. M (mmol)[a]	Amine Conc. M (mmol)	Temp. (°C)	TF[a]	Time (h)	H_2 Produced (mmol)
0.97 (14.6)	0.31 (4.6)	180	11.3	10.0	6.4
3.7 (55.6)	0.31 (4.6)	180	13.7	10.5	10.4
3.7 (55.6)	0.31 (4.6)	200	23.6	9.3	12.2
5.6 (83.3)	0.31 (4.6)	180	14.1	10.2	(6.9)
0.97 (14.6)	0.61 (9.2)	180	12.3	7.6	6.0
1.8 (27.8)	0.61 (9.2)	200	24.2	6.5	10.4
3.7 (55.6)	0.61 (9.2)	180	19.0	10.2	7.8
3.7 (55.6)	0.61 (9.2)	200	27.1	8.5	11.1
5.6 (83.3)	0.61 (9.2)	180	21.3	9.8	9.8
5.6 (83.3)	0.61 (9.2)	200	29.3	10.2	15.1
7.4 (111.0)	0.61 (9.2)	180	19.0	13.6	10.0
7.4 (111.0)	0.61 (9.2)	200	25.9	11.4	15.5
5.6 (83.3)[c]	4.1 (62.1)	180	56.2	4.9	14.7
5.6 (83.3)[c]	4.1 (62.1)	200	48.0	4.9	12.9

[a]Conditions: 0.1 mmol $Ru_3(CO)_{12}$, N,N,N',N'-tetramethyl-1-6-hexanediamine, volume increased to 5 mL with triglyjme, 1 mg (0.018 mmol) NaSH, 360 psi.

[b]TF = turnover frequency (mmol H_2/mmol catalyst/hour).

[c]No other organic solvent.

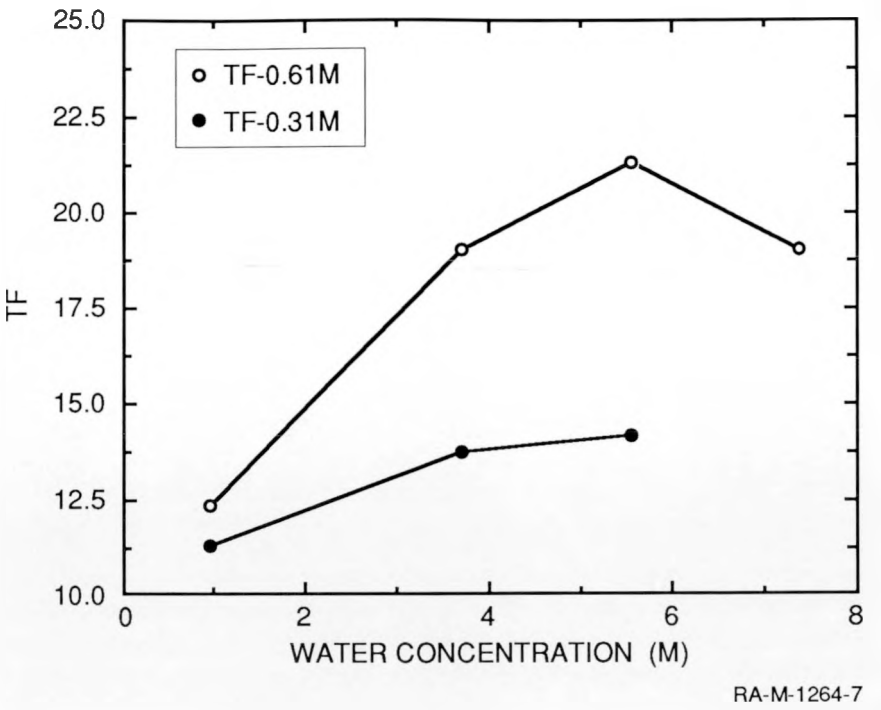

Figure 4. Ru-catalyzed WGSR rate versus water concentration.

(0.31, 0.61 M amine)

We also looked at the $Mo(CO)_6/K_2CO_3$/triethylene glycol system WGSR rate as a function of water concentration (see Table 13). The TF increases to a maximum at 5.56 M (83.3 mmole) water with NaSH (14.7) or without NaSH (22.9). The amount of hydrogen produced continued to increase only very slowly above 5.56 M H_2O and there was little variation in reaction time. The 64% rate reduction for $Mo(CO)_6$ with the small amount of added NaSH agrees with results reported by King.[92] He found that when Na_2S was used as *base* instead of KOH with $Mo(CO)_6$, the rate was 63% slower (TF of 36.2 versus. 22.9). Not surprisingly, added NaSH had very little effect on the total hydrogen produced.

Catalyst Concentration

We also studied the dependence of catalyst activity on Mo concentration under batch conditions to gain an understanding of appropriate catalyst concentrations for the continuous-flow system. We found that changing the amount of $Mo(CO)_6$ present in our system did not appreciably affect the rate (expressed as mmol H_2/h). These data are presented in Figure 5 (where the lower two points on the rate scale were taken at 180°C and the other 4 at 200°C). The values of TF increased markedly as the catalyst concentration

was decreased, which suggests that this catalyst system operates most efficiently at low Mo concentrations. This result, however, also meant that the rate of hydrogen production showed little dependence on the amount of added Mo

Table 13. $MO(CO)_6$-CATALYZED RATE VERSUS WATER CONCENTRATION

	Water Conc. M (mmol)[a]	TF[b]	Reaction Time (s)	H_2 Produced (mmol)
Without NaSH[a]	1.8 (27.8)	10.5	10.2	6.9
	3.7 (55.6)	15.3	9.8	10.8
	5.6 (83.3)	22.9	9.9	12.6
With NaSH	3.7 (55.6)	9.6	12.2	9.9
	5.6 (83.3)	14.7	11.6	12.4
	7.4 (111.0)	14.3	11.5	12.5

[a]$Mo(CO)_6$ (0.1 mmol), 0.15 g (1.08 mmol) K_2CO_3, 200°C, triethylene glycol to a volume of 15 mL, 1 mg (0.018 mmol) NaSH, 360 psi.

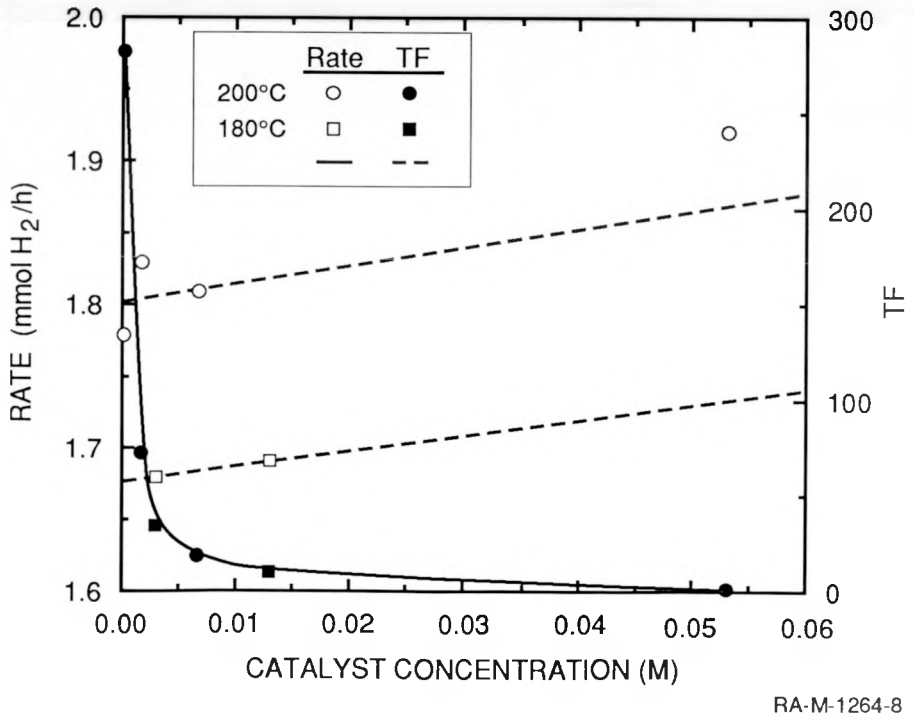

Figure 5. WGSR rate versus $Mo(CO)_6$ concentration.

(at the same temperature the rate varied less than 20% over two order of magnitude in catalyst concentration).

CONTINUOUS-FLOW REACTOR WITH RECYCLE

Following the batch reactor studies, which demonstrated that several of the homogeneous catalysts were sulfur tolerant, had activity closer to equilibrium than previous laboratory studies, and served to give a preliminary ranking of catalysts to pursue, the next technical task was to measure activity under continuous-flow conditions to input to the economic model. We decided to study both Mo and Ru based catalysts in more detail based on the results of the batch studies, but to concentrate on Mo because of the lower catalyst cost. We first designed a test to determine whether either catalyst system would show sufficient longevity to be used in a continuous-flow reactor. The lifetime of the ruthenium catalyst was tested by running later runs with the same solution in the batch reactor. The gas mixture was replenished in the bomb before each run and the TF were observed to decline (see Table 14). However, loss of water was suspected; therefore, the test was rerun with 0.25 ml of water added after each run and the TF remained constant (TF = 12.7 ± 0.8).

Table 14. RATES FROM A $Ru_3(CO)_{12}$-CATALYZED WGSR SYSTEM WITH DAILY INTRODUCTION OF GASEOUS REAGENTS[A]

Run	TF w/o added H_2O	TF with added H_2O[b]
1	13.7	12.4
2	10.4	11.8
3	6.1	13.8
	TF average =	12.7

[a]0.1 mmol $Ru_3(CO)_{12}$, 1.0 mL (4.6 mmol) tetramethyl-1,6-hexanediamine, 1.0 mL (55.6 mmol) H_2O, 13.0 mLtriglyme, 1 mg (0.018 mmol) NaSH, 360 psi, 180°C.
[b]0.25 mL (13.9 mmol) H_2O added between runs.

Table 15 shows that the $Mo(CO)_6/K_2CO_3$ catalyst system, like that based on $Ru_3(CO)_{12}$, loses no activity over at least 4 days under our batch conditions when the gas mixture within the bomb is replenished once daily (6.67×10^{-3} M $Mo(CO)_6$, 0.362 M K_2CO_3,

180°C, 1000 ppm NaSH, 7.41 M H_2O, triethylene glycol to a total volume of 15 mL, TF = 18.1 ± 2.5). These results suggested that both catalyst systems would have a significant lifetime under continuous-flow conditions.

Table 15. RATES FROM A $MO(CO)_6$-CATALYZED WGSR SYSTEM WITH DAILY INTRODUCTION OF GASEOUS REAGENTS[a]

Run	TF
1	15.8
2	22.3
3	17.2
4	17.2
TF average =	18.1

[a] 6.67×10^{-3} M $Mo(CO)_6$, 0.362 M K_2CO_3, 180°C, 1000 ppm NaSH, 7.41 M H_2O, triethylene glycol to a total volume of 15 mL.

We found that the results of varying the Mo concentration in the continuous-flow studies were similar to those of the batch studies. As in the batch studies, the value of TF did increase with decreasing Mo concentration, but the rate of hydrogen production remained constant. Plots of TF versus. catalyst concentration, shown in Figure 6 for two concentrations of K_2CO_3, suggest that we will be unable to increase hydrogen output rate by increasing catalyst concentrations in this system.

We next studied the effect on catalyst activity of variations in the concentration of base and found that turnover frequencies in the continuous-flow system vary little with base concentration. In a batch reaction that had a Mo concentration of 3.33×10^{-3} M, the TF for H_2 decreased 2.7-fold, from 28.0 to 10.4 mmol H_2/mmol Mo/h, when the concentration of base was decreased by a factor of 6.8, from 0.072 M to 0.493 M. In the continuous-flow study, three base concentrations were examined with a Mo concentration of 6.67×10^{-3} M. The TF values for CO consumption at 0.362, 0.181, and 0.0905

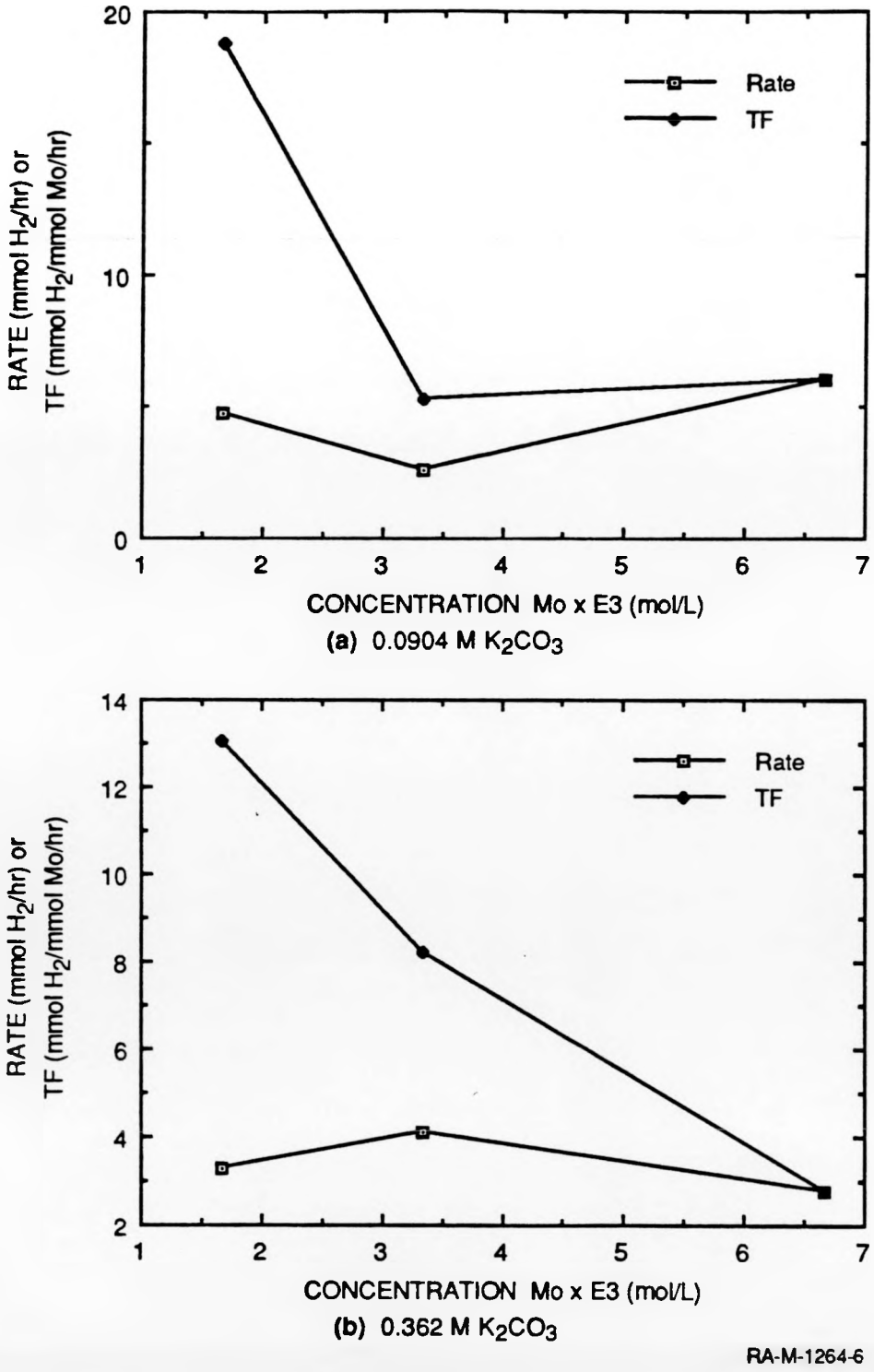

FIGURE 6. Turnover frequency and rate of hydrogen production versus catalyst concentration, continuous-flow mode.

M K_2CO_3 did not vary significantly (9.29, 8.43, and 8.73 mmol CO/mmol Mo/h, respectively), which suggests that catalyst activity is fairly insensitive to base concentration in the continuous-flow system. Our data have allowed us to conclude that the dependence of the rate of hydrogen production on K_2CO_3 concentration is less than first-order under both batch and continuous-flow conditions.

An alternative to increased catalyst concentration as a means of increasing product yields is to increase the flow rate of input gases and/or the concentrations of reactant input gases. Our highest value of TF in this system, 92.8 mole CO/mole Mo/h, was obtained with a solution that was 2.5×10^{-4} M in Mo and 0.0905 M in K_2CO_3 and had a feed gas flow rate of 40 mL/min, twice our standard value.

During a reaction that was 2.5×10^{-4} M Mo and 0.0905 M K_2CO_3 with a feedgas flow rate of 20 mL/min, we varied the water flow rate from 0.005 mL/min to 0.020 mL/min. The results (as plotted in Figure 7) are that the WGSR rate goes through a maximum relative to water flow rate within this range.

We ran two reactions in the continuous-flow reactor from which we hoped to obtain kinetic and mechanistic information regarding our molybdenum-catalyzed homogeneous WGSR. Under standard conditions (0.264 g $Mo(CO)_6$, 1.875 g K_2CO_3, 150 mL triethylene glycol, 0.005 mL/min liquid H_2O, 200°C, 320 ± 20 psi, stir rate of 1420 rpm), the input flow rates of CO and H_2 were varied in separate experiments. The input flow rate of our standard feedgas mixture was kept at 20 mL/min while the flow rate of additional CO was varied between 0 and 33 mL/min or the flow rate of additional H_2 was varied between 0 and 29.4 mL/min in the CO and H_2 variation experiments, respectively.

Figures 8 and 9 plot the rates of CO consumption and CO_2 production as a function of time for the experiments in which CO and H_2 were varied, respectively. Each section of these graphs shows the factor by which the amount of CO or H_2 in the input stream was raised above that present in the feedgas stream alone (= 1.0) during that time period. The linearity of the graph in all sections during the CO variation experiment, except near times at which changes in flow rate were made, reveals that the steady-state consumption of CO and production of CO_2 do not vary with CO concentration over the range of CO mole fractions used. The average values of the steady-state rates (22 out of 90 points) of CO consumption and CO_2 production during the CO variation experiment were 12.9 mmol/h and 13.0 mmol/h, respectively.

Although the plot of CO consumption and CO_2 production versus. time for the H_2 variation experiment shows more scatter in steady-state rates than for the CO variation

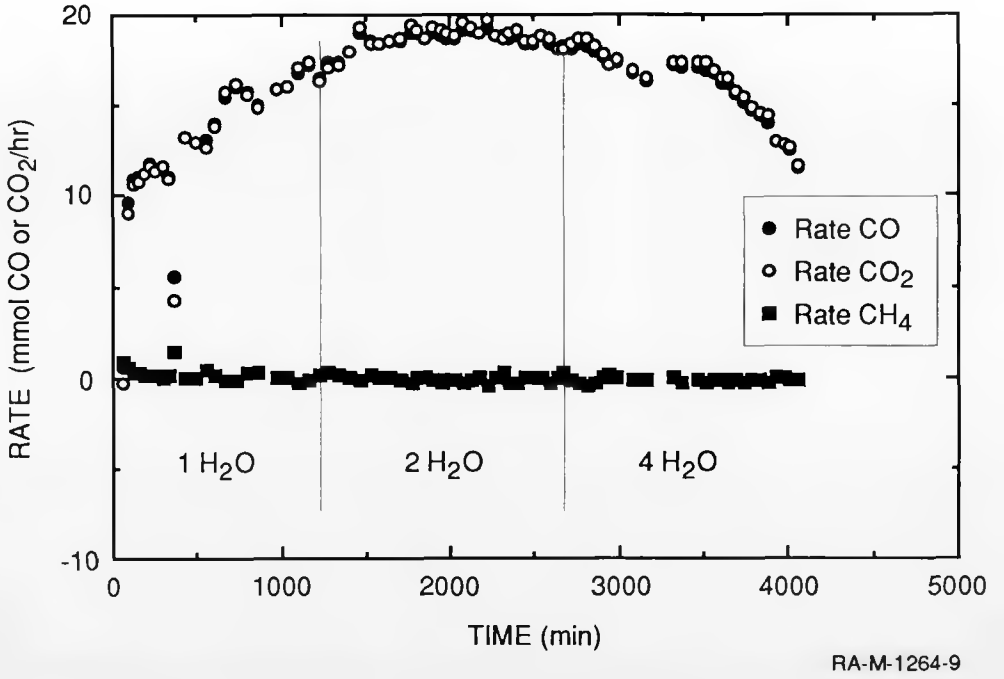

FIGURE 7. Rate of $Mo(CO)_6$-catalyzed WGSR versus water flow rate, continuous-flow mode.

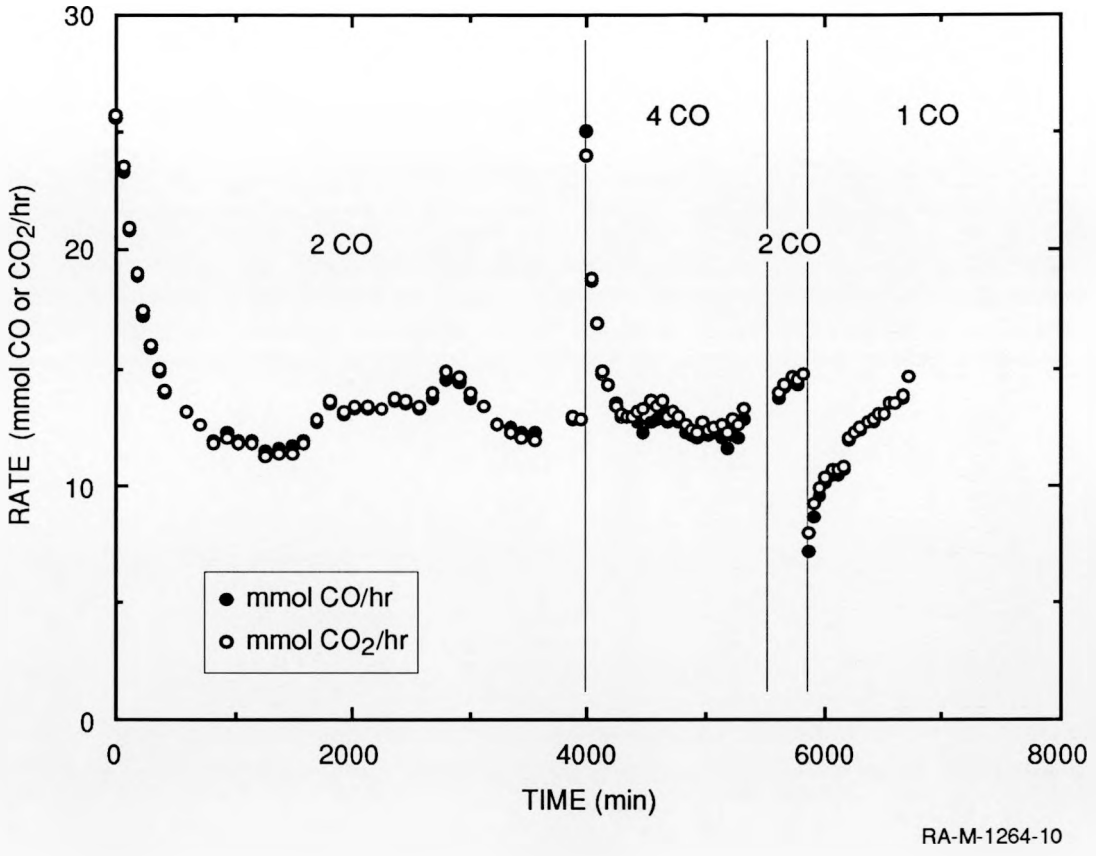

Figure 8. CO consumption and CO_2 production as a function of CO flow rate.

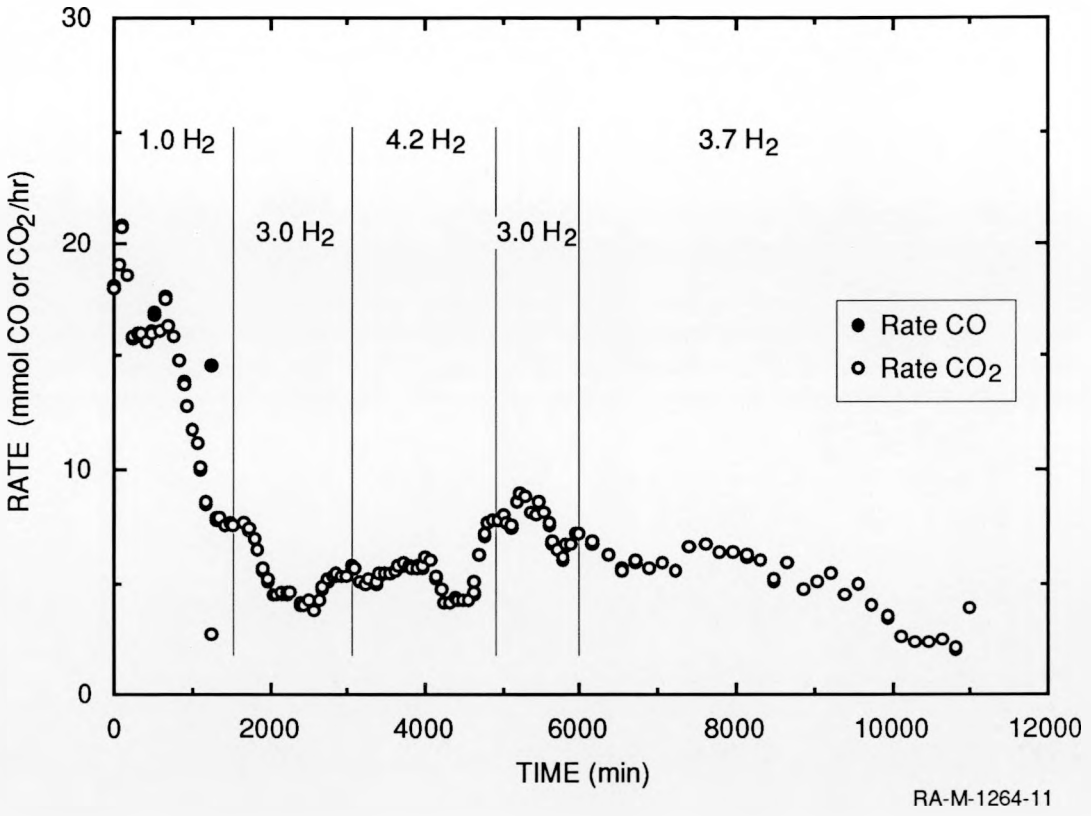

Figure 9. CO consumption and CO_2 production as a function of H_2 flow rate.

experiment, it does suggest that the rates of CO consumption and CO_2 production are independent of H_2 concentration over the range of H_2 mole fractions used. The average values of the steady-state rates (95 out of 128 points) of CO consumption and CO_2 production during the H_2 variation experiment were 5.9 mmol/h and 5.6 mmol/h, respectively.

Our initial studies with $Ru_3(CO)_{12}$ in the continuous-flow reactor showed unexpectedly low values of TF (31 mole H_2/mole Ru/h with a Ru_3 concentration of 2.5 x 10^{-4} M), but this system is complicated by side reactions such as disproportionation of the N,N,N',N'-tetramethyl-1,6-hexanediamine solvent.

DISCUSSION

SCREENING OF CATALYSTS

Catalysts that appear likely to have reasonable activities in the presence of sulfur from our review of the literature were further screened based on three other guidelines:

- Cost of catalyst. Cost eliminated all third-row metals except for tungsten and made rhodium a borderline choice. For example we eliminated the $Rh(PPr^i_3)_3$ catalysts of Yoshida et al.[24,33] because these catalysts are expensive to synthesize and to handle.

- Corrosive conditions. We eliminated from consideration any of the homogeneous WGSR catalysts that have reasonable activities only under extreme conditions, which we defined as pH 2 or less and pH 11 or more.

- Volatile solvents and promoters (e.g., low boiling alcohols and amines).

These guidelines led us to choose the following ten catalysts for the initial screening portion of the study:

Catalysis 1-3: King demonstrated that the group 6 metal carbonyls [$Cr(CO)_6$, $Mo(CO)_6$, and $W(CO)_6$] are active in alcoholic base containing considerable amounts of sulfide.[88,92] These were studied with low boiling alcohols and alkali formate as the base. Therefore, these catalysts were tested with high boiling alcoholic solvents and alkali bases.

Catalysis 4: The simple $Ru_3(CO)_{12}$/alcohol/hydroxide system was also shown by King to be sulfur tolerant.[88,92] We have examined this system in great detail previously and used this system as the standard for gauging other catalysts tested.

Catalysis 5: Mixed-metal catalysts such as $Fe(CO)_5/Ru_3(CO)_{12}$/ alcohol/hydroxide have been examined under many conditions previously and have exceptionally high activities. King found that the iron carbonyl catalyst deactivates in the presence of sulfur,[88,92] and Ford observed that the mixed-metal catalyst was susceptible to poisoning by sulfur.[12]

Catalysis 6: We have previously observed that the ruthenium/ amine systems are likely to suffer from degradation and/or volatility of the amine. In other studies we observed that methyl amines such as N,N'-dimethylpiperazine and tetramethylethylene diamine are more stable in the presence of $Ru_3(CO)_{12}$ under CO. However, these catalysts have

the highest rates reported in the literature for homogeneous catalysts. Therefore, this catalyst system was tested using a high boiling amine.

Catalysis 7: The work of Marnot et al.[72] indicates that rhodium/ sulfonated phenanthroline WGSR systems are quite active. Therefore, we tested such a system as a candidate catalyst for a sulfur/tolerant WGSR catalyst.

Catalysis 8: The work of Alessio et al.[74] suggests that the related ruthenium/sulfonated phenanthroline systems could be an effective WGSR catalyst. We tested the sulfur tolerance of this system.

Catalysis 9: Marnot et al.[72] mentions, without details, that the cobalt/sulfonated phenanthroline complexes also catalyze the WGSR. Thus we included this system in our screening plan.

Catalysis 10: The work of Kaspar et al.[82] with the meta-monosulfonated triphenyl phospine complexes of rhodium gives a catalyst that is extremely active at pH = 2 (TF = 127). Although the acidity is quite high, the activity was so high relative to the other rhodium catalysts that this system must be included on the list of catalysts to be screened.

The results of the initial screening in batch reactors under realistic WGS conditions (simulated oxygen blown coal gas and sulfur as described in the experimental section) are shown in *Table 9 on page 48*. Under these conditions the most active catalyst was ruthenium carbonyl with an amine base. Wheng N,N,N',N'-tetramethyl-1,6-hexanediamine was used as the base the ruthenium catalyst produced 86 mmol H_2/mmol catalyst/h (TF = 86). The next most active catalyst was the molybdenum carbonyl with alkali base in alcoholic solvent, which had a TF of 28 under these batch conditions. The maximum TF reported in the literature for ruthenium are the 330 (THF solvent, trimethylamine base, 100°C, 23.8 atm CO) reported by Kang et al.[9] and the 574 TF (diglyme solvent, trimethylamine base, 100°C, 51 atm CO) reported by Slegeir et al.[52]

In contrast to the ruthenium results, where our turnover frequencies are much lower than the literature values, our results for group 6 catalyzed reactions are much higher than those reported in the literature. The highest reported rate for a molybdenum catalyst was TF = 9 reported by Haenel et al.[93] (aqueous solutions, KOH, 250°C, 45 atm CO). The highest values in the presence of sulfur reported in the literature are those reported by King et al.[92] who reported 2.5 TF for $Cr(CO)_6$, 5.4 TF for $Mo(CO)_6$, and 7.5 TF for $W(CO)_6$ (MeOH solvent, NaSH as the only base, 160°C, 27.2 atm CO). Their sulfide-promoted results are in sharp contrast to those they reported earlier for hydroxide-promoted WGS by group 6 metal carbonyls where chromium was the most active TF =11.7, tungsten was

next at TF = 5.8, followed by molybdenum at TF = 5.4 (MeOH solvent, KOH base, 140°C, 7.8 atm CO).[92]

Our results, which show molybdenum to be the most active of the group 6 metals in the presence of both sulfur and an additional base promoter, are not in agreement with either of their results: molybdenum TF = 28, chromium TF = 12, and tungsten TF = 4.2 [triethylene glycol solvent, K_2CO_3 base (with 1% NaSH), 180°C, 30 atm coal gas]. In addition, in some cases, we were able to observe significantly higher rates such as when KOH was used as a base at low concentrations where we observed a TF of 41.8. Our maximum turnover frequency was observed at very low catalyst concentrations where TF > 250 (*see Figure 5*).

These screening studies demonstrated that several of these homogeneous catalysts are highly sulfur-tolerant and maintain activity under the more realistic conditions of coal gas feed and high boiling solvents, but they perform under these more realistic conditions differently than reported in the literature: molybdenum is more active than reported and ruthenium is less active.

CONTINUOUS-FLOW TESTS

The screening studies in batch reactors demonstrated that the ruthenium catalyst, followed by the molybdenum, were the most active catalysts and worthy of more detailed examination. Industrially, the WGS process must run continuously, so the next stage in the development was to evaluate the usefulness of these catalysts for a continuous process. Important issues to be addressed when running the reaction continuously include the stability of the catalyst, the effect of promoter and reagent concentrations.

One of the primary concerns with operation of the WGS process continuously is the stability of the catalyst. We have previously shown that transalkylation reactions of tertiary amines are catalyzed by $Ru_3(CO)_{12}$.[53] This behavior would affect the stability of the WGS reaction by consuming the amine base to produce the volatile amine NMe_3 (reaction 54).

$$Me_2N(CH_2)_6NMe_2 \xrightarrow{Ru_3(CO)_{12}} Me_3N + Me_2N(CH_2)_6N(Me)(CH_2)_6NMe_2 \quad (54)$$

Mass spectral analysis of a reaction solution from the screening studies in the batch reactor after 20 h indicated that approximately 10% of the remaining amine was the triamine ($Me_2N(CH_2)_6N(Me)(CH_2)_6NMe_2$).

However, the transalkylation reaction does not appear to cause catalyst stability problems in the batch reactor. We ran successive 20-h reactions with the same catalyst charge, but replenishing the reactants and got the same reaction rate (*see Table 14, page 57*). We ran the same experiment with the molybdenum catalysts with the same results (*see Table 15, page 58*).

The superior reaction rates observed with the $Ru_3(CO)_{12}$ catalyst are promising, but the activity of this catalyst exhibits considerable variation with respect to the reaction environment. The highest rate observed of 86 mmol H_2/mmol catalyst/h was observed in the absence of solvent: the catalyst was just dissolved in a mixture of water and amine base. The fastest observed rate in the presence of a solvent was less than TF = 30. The rate in aprotic solvents (triglyme) were considerably greater than those observed in protic solvents (triethylene glycol). Water concentration has very little effect on the activity except that the activity drops at high water concentrations. For example, in neat amine base TF = 86 was observed with 3.7 M water and TF = 56 was observed when the water concentration was increased to 5.6 M.

We observed less variability in the results for the catalytic system of molybdenum carbonyl in alcoholic solvent with alkali base. The effects of base concentration are shown in Table 16 where at reasonable concentrations the most effective base is K_2CO_3, but at low concentrations KOH gave the highest rate, TF = 41.8. Water concentration also had only a very small effect on the rate, going through a maximum at 5.6 M.

Table 16. EFFECT OF ALKALI BASE[A]

Base	Conc. (M)	TF
K_2CO_3	0.072	10.4
KOH	0.072	41.8
KO_2CH	0.493	8.8
K_2CO_3	0.494	28.0
KOH	0.493	23.6

[a](0.1 mmol $Mo(CO)_6$, 55.6 mmol H_2O, 180°C, 1000 ppm NaSH, triethylene glycol.

We observed an unusual effect of catalyst concentration where the rate of hydrogen production is independent of catalyst concentration (*Figure 5, page 56*). Thus at high Mo concentrations we observed very low TF, and at low Mo concentrations we observed very high TF (exceeding 250). However, the rate of hydrogen production remained relatively constant at about 2 mmol H_2/h (from 15 mL of solution; corresponds to 0.13 mol H_2/liter of solution/h).

We chose to concentrate our studies in the continuous-flow reactor on the molybdenum based catalysts because of the potential stability problem of the ruthenium catalyst system using alkyl amine base, because at an identical concentration of ~7 x 10^{-3} M the molybdenum catalyst actually demonstrates higher rates in our batch reactor at 180°C (18 versus 12), and because of the relative cost of the metal carbonyl catalyst precursor.

The continuous-flow experiments were conducted in a stirred tank reactor of 300 mL with 150 mL loading of solution. The dead gas is recycled using an impellor. The gas input/output is typically 20 mL/min, which leads to a gas holdup time of approximately 10 minutes. The reactors were typically started by loading in air, then heated to temperature while purged with dry simulated coal gas. The H_2O is introduced at temperature and the time of it introduction is designated as time zero for the reactions.

We found that the results of varying the Mo concentration in the continuous-flow studies were similar to those of the batch studies. As in the batch studies, the value of TF did increase with decreasing Mo concentration, but again plots of rate of hydrogen production and TF versus. catalyst concentration, shown in Figure 5 (page 56) for two concentrations of K_2CO_3, suggest that we will be unable to increase hydrogen output by increasing catalyst concentrations in this system.

We next studied the effect on catalyst activity of variations in the concentration of base and found that turnover frequencies in the continuous-flow system vary little with base concentration.

An alternative to increased catalyst concentration as a means of increasing product yields is to increase the flow rate of input gases and/or the concentrations of reactant input gases. Our highest value of TF in this system, 92.8 mole CO/mole Mo/h, was obtained with a solution that was 2.5 x 10^{-4} M in Mo, 0.0905 M in K_2CO_3, and had a feed gas flow rate of 40 mL/min.

King et al.[92] proposed the mechanism described in Scheme 20 for the molybdenum catalyzed WGS:

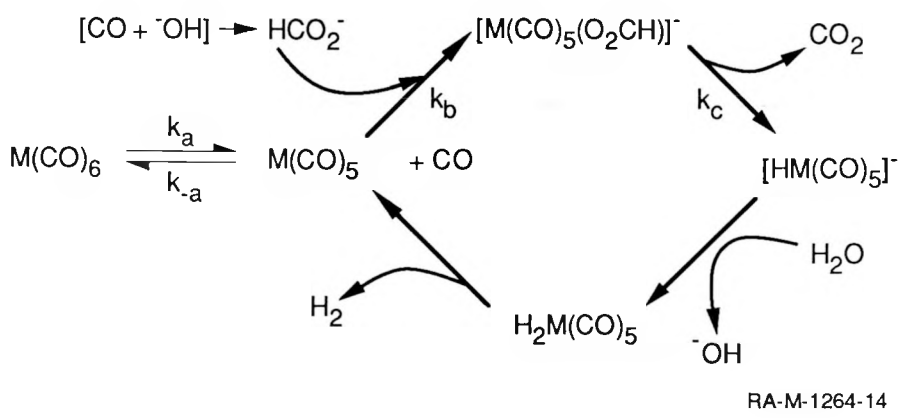

SCHEME 20

King reported a different mechanism for group VIII metal catalysis of the WGS (particularly $Fe(CO)_5$), which is shown in Scheme 21).

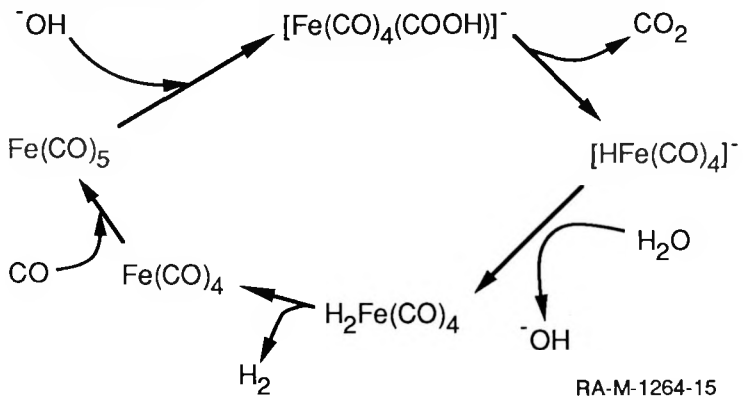

SCHEME 21

The kinetic data that lead King to these conclusions are listed in Table 17.

Table 17. COMPARISON OF CATALYST SYSTEMS DERIVED FROM $Fe(CO)_5$ AND $M(CO)_6$ (M-Cr, MO, W)

(from King et al. ACS Symp. Ser. 1981, 152, 123)

	$Fe(CO)_5$	$Cr(CO)_6$	$Mo(CO)_6$	$W(CO)_6$
Optimum solvent composition (% H_2O, V/V in methanol)	25	10	10	10
Rate dependence on metal carbonyl concentration	First order	First order	First order	First order
Rate dependence on carbon monoxide pressure	Zero order	Inverse first order	Inverse first order	Inverse first order
Rate dependence on added base (formate) concentration	Zero order	Approximately first order	Approximately first order	Approximately first order
Temperature dependence of rate expressed as activation energy (kcal/mole)	22	35	35	32
Minimum CO pressure required to maintain catalyst activity (atm)	3-7	none	none	none
Catalytic activity in presence of sulfide ion (expressed as percent of activity under sulfur-free conditions)	none	21	59	67

Darensbourg and Rokicki[94] also studied the molybdenum-catalyzed WGS reaction and concluded that the mechanism was more like that King et al.reported for the iron-catalyzed reaction involving metallocarboxylate intermediates (Scheme 22).

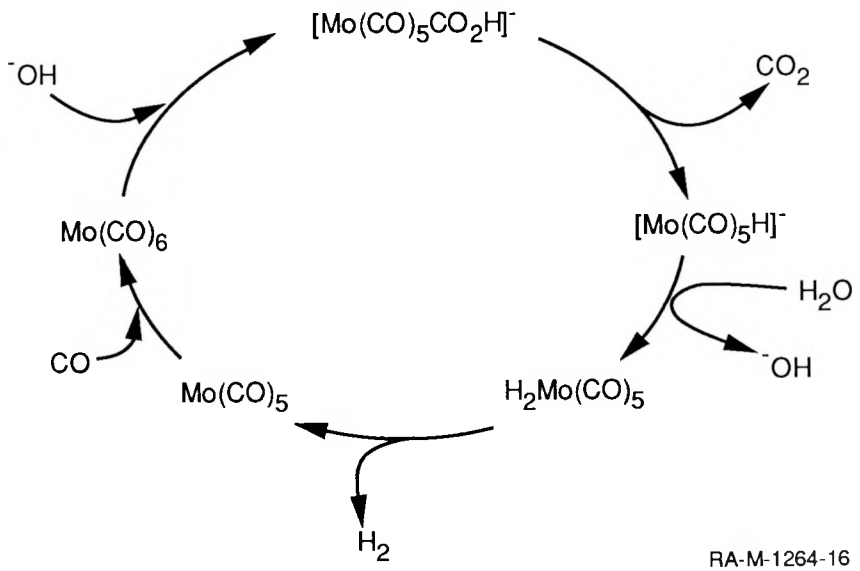

SCHEME 22

They base their argument on three critical points. First, the equilibrium between the metalloformate and free CO_2 lies far toward the metalloformate.[28]

$$[M(CO)_5H]^- + CO \rightleftharpoons [Mo(CO)_5CO_2H]^- \qquad K_{eq} >> 1$$

Second, the rate of formate formation from carbon monoxide and hydroxide is much slower than the rate of metallocarboxylate formation from metal carbonyl and hydroxide (5 to 6 orders of magnitude).[19] And third, the activation energies determined by King et al. are lower than the activation energies for CO dissociation from these carbonyls (King data shown in Table 17; BDE[95] Cr = 37, Mo = 40, and W = 46 kcal/mol). The key data in support of King's mechanism are their measured first-order dependence on formate

concentration and inverse dependence on carbon monoxide pressure. These mechanistic differences have never been completely resolved, but the possibility exists that both mechanisms are active depending on the base used and the other reaction conditions.

Our data, in both the batch and continuous-flow reactors, is more consistent with Darensbourg's mechanism. We see in both reactors an approximately zero-order dependence on base concentration (when using K_2CO_3), and in the batch reactor the dependence appears to go through a maximum. In the batch reactor, the effect of different bases (potassium formate and potassium hydroxide) was also checked: formate showed much lower rates, while KOH showed higher rates only at very low concentrations. The effect of carbon monoxide concentration was checked only in the continuous-flow reactor where it was found to have no effect on the rate. Although these data are more consistent with the metallocarboxlate mechanism than the metalloformate, it should also be pointed out that we observed a zero-order dependence on catalyst concentration which is not consistent with either mechanism. Such an effect has been reported previously in the WGSR literature[67,96] and has been explained as catalyst saturation kinetics.[96]

In both the batch and continuous-flow reactors, we observed a maximum in the rate with respect to water concentration. This maximum is consistent with the data reported by King et al. Grant explained this by showing that water can occupy a coordination site on the metal and therefore slow the loss of CO_2 (because a vacant site is required for decarboxylation).[58]

We observed inequalities between the conversion of CO and the yields of H_2 and CO_2 in many of our runs, with conversion of CO typically higher than the yield of H_2 and CO_2. These differences also appear in most literature reports of the WGSR over both homogeneous and heterogeneous catalysts where raw data are given.[67,97] Over heterogeneous catalysts, this difference is usually explained as being the result of side reactions leading to hydrocarbon (or alcohol) products (since many of the WGS catalysts are also FTS or methanol catalysts).[97] We looked carefully for evidence of hydrocarbon or alcohol products in our reaction solutions without finding any. In the continuous-flow reactor, we measured methane and observed no production (see Figure 7, page 61).

ECONOMIC EVALUATION

The experimental results discussed above formed the basis for a preliminary process design and economic evaluation of the homogeneous catalyst in terms of a proposed plant design based on the reaction model, current costs, and standard chemical engineering practice. The design and evaluation incorporates a homogeneous LT shift catalyst into a coal gasification plant for making 1,000 ton/day hydrogen. We compared the evaluation of such a plant with an integrated plant that uses a standard heterogeneous HT shift plus a heterogeneous LT shift to establish the economic advantages or disadvantages of the homogeneous WGSR system.

The shift reaction is a small but critical portion of the process for manufacturing hydrogen. It is especially important for the manufacture of hydrogen from coal. The Texaco coal gasifier produces a gas that contains about 51.9 mol% carbon monoxide and about 35.3 mol% hydrogen. By the addition of water, however, more hydrogen can be produced as CO is converted to CO_2:

$$H_2O + CO \longrightarrow H_2 + CO_2 \qquad (54)$$

This is the water-gas shift reaction. On an industrial scale, the heterogeneous reaction is catalyzed by mixtures of iron and chromium oxides at 350°C or higher (high-temperature shift, or HTS). Equilibrium is reached at 80% to 85% conversion, and the reactor products are customarily passed to a second heterogeneous catalyst that operates at lower temperatures (about 200°C) at which the equilibrium favors over 95% complete reaction of the CO to CO_2 and hydrogen (low-temperature shift, or LTS). Low-temperature shift is not suitable alone because the reaction is too slow. (More active LTS catalysts such as mixtures of zinc and copper oxides are sensitive to poisoning by sulfur compounds and can be used only if the coal or the gasifier product is desulfurized before the WGSR step.)

There has, therefore, been considerable interest in developing homogeneous catalyst systems that are sulfur-tolerant and that would show sufficient activity at low

temperatures to permit a one-stage shift reaction for hydrogen production. Although laboratory work to date has not yet demonstrated a sufficiently active homogeneous catalyst system, we made a preliminary evaluation of some the costs associated with a hypothetical plant to show the performance that would be required for a plant based on a hypothetical homogeneous WGSR to compete successfully with a typical plant that uses a conventional heterogeneous WGSR.

DESCRIPTION OF THE INTEGRATED COAL-TO-HYDROGEN PLANT

The complete coal-to-hydrogen plant with a hypothetical homogeneous WGSR catalyst is shown in the block flow diagram of Figure 10. Compositions and flow rates of key streams in a plant to produce 1000 tons/day of hydrogen (300,000 metric tons/yr) are tabulated in Table 18.

Coal Storage, Preparation, Grinding, and Slurrying

Washed Illinois No. 6 bituminous coal (3.2 wt% sulfur) is delivered to the plant in unit trains of 100-ton bottom-dump cars. The coal is unloaded by conveyors, checked for metal fragments, and stored in piles. A hammer mill crushes the pieces of coal, some of which may be as large as 1.5 inches, to less than 0.75 inch. Conveyors are fitted with water sprays to suppress dust.

Four parallel lines are used for coal grinding and slurrying. The crushed coal is fed from storage to a two-stage grinding unit, where the coal is pulverized so that 80% of it passes through a 200-mesh screen. Ground coal is slurried with recycled process water and makeup water to produce a 60 wt% solids coal slurry. The coal slurry is pumped to the gasifiers.

Air Separation

Oxygen of 98% purity is produced by air separation in three 2417-tons/day units. Air feed is compressed in two-stage axial/centrifugal compressors driven by condensing steam turbines using high-pressure steam. Oxygen product is compressed in centrifugal compressors driven by condensing steam turbines using high-pressure steam. Some of the co-product nitrogen is compressed (electric motor) and used in the acid gas removal section.

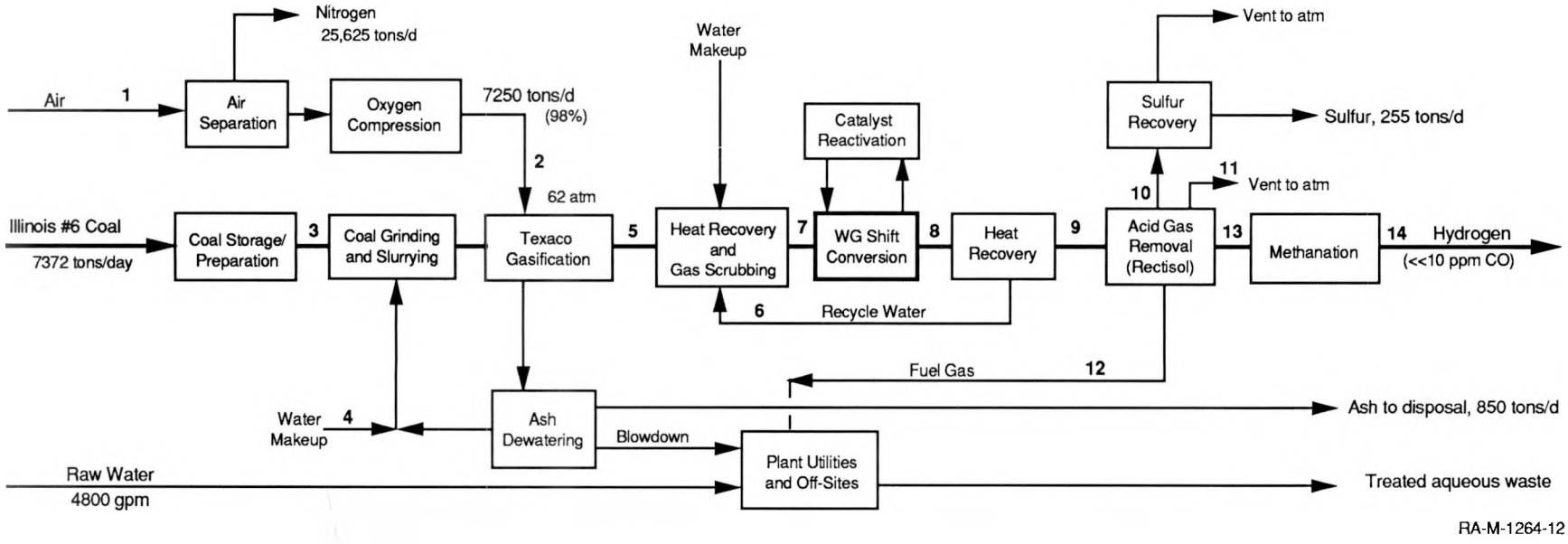

FIGURE 10. Hydrogen from coal: block flow diagram.

Table 18

HYDROGEN FROM COAL--MATERIAL BALANCE

		1 Air to Cryo Plant		2 O2 to Gasifier		3 Coal to Coal Prep	4 Makeup Slurry Water		5 Gasifier Product		6 Quench/Scrub Water		7 To Shift Conversion	
	MW	lb-mol/h	lb/hr	lb-mol/h	lb/hr	lb/hr	lb-mol/h	lb/hr	lb-mol/h	lb/hr	lb-mol/h	lb/hr	lb-mol/h	lb/hr
Hydrogen	2								18,924	38,151			18,924	38,151
Carbon Monoxide	28								25,645	718,046			25,645	718,046
Carbon Dioxide	44								9,782	430,396			9,782	430,396
Methane	16								197	3,148			197	3,148
Oxygen	32	19,566	626,115	18,431	589,800									
Nitrogen	28	72,675	2,034,911	58	1,632				327	9,158			327	9,158
Argon	40	913	36,528	308	12,338				308	12,318			308	12,318
Hydrogen sulfide	34								624	21,233			624	21,233
Carbonyl sulfide	60								40	2,384			40	2,384
Coal						543,538								
Ash						70,837								
Water	18	2,334	42,007				7,200	129,609	36,143	650,572	95,486	1,718,744	121,043	2,178,777
		95,488	2,739,560	18,798	603,770	614,375	7,200	129,609	91,989	1,885,407	95,486	1,718,744	176,889	3,413,612

		8 Chilled Shifted Gas		9 Feed to CO2 Removal		10 Gas to S Recovery		11 Tail Gas Vent to Atm		12 Fuel Gas from Rectisol		13 Feed to Methanation		14 Hydrogen Product	
	MW	lb-mol/h	lb/hr	lb-mol/h	lb/hr	lb-mol/h	lb/hr	lb-mol/h	lb/hr	lb-mol/h	lb/hr	lb-mol/h	lb/hr	lb-mol/h	lb/hr
Hydrogen	2	44,343	89,396	44,343	89,396	33	66	58	116	1,673	3,374	42,579	85,839	41,544	83,753
Carbon Monoxide	28	225	6,313	225	6,313	0	10	5	144	47	1,314	173	4,844		
Carbon Dioxide	44	35,201	1,548,835	35,164	1,547,220	2,006	88,273	29,881	1,314,758	3,148	138,513	129	5,676		
Methane	16	197	3,148	197	3,148			19	304	54	861	124	1,984	426	6,816
Oxygen	32														
Nitrogen	28	327	9,158	327	9,158	33	912	3,430	96,049	3	92	345	9,660	345	9,660
Argon	40	308	12,318	308	12,318			1	40	5	198	302	12,080	302	12,080
Hydrogen sulfide	34	656	22,314	656	22,314	656	22,310	0	3						
Carbonyl sulfide	60	8	477	8	477	8	469	0	8						
Coal															
Ash															
Water	18	95,624	1,721,234	138	2,490							20	360	51	918
		176,889	3,413,192	81,367	1,692,833	2,736	112,040	33,394	1,411,423	4,930	144,352	43,672	120,443	42,668	113,227

Coal Gasification and Ash Handling

Four parallel lines are used for coal gasification and ash handling. In the Texaco process, the coal-water slurry is fed, together with oxygen, through special burners into a vertical gasification reactor. The top burners feed downward into a refractory-lined chamber, where partial combustion takes place at 915 psig and 2300°-2800°F. The product gas consists primarily of CO, H_2, CO_2, and steam. Most of the sulfur in the coal is converted to H_2S, the rest to COS. The product is essentially free of uncombined oxygen. The product contains some unconverted carbon and all the ash, in the form of molten slag.

A small portion of the gas formed in the gasifier passes straight down into the bottom section of the gasifier, carrying with it most of the larger slag particles, which are quenched with water and discharged via a lock-hopper. The ash is dewatered mechanically and sent to disposal. Water recovered from the ash is recycled to the slag quench and coal slurrying units. A bleed stream of this water is purged to a treating unit to prevent buildup of ultrafine solids, dissolved metals, ammonia, and traces of other impurities.

Gas Scrubbing and Heat Recovery

Four parallel lines are used for gas scrubbing and heat recovery. Leaving the molten slag behind, the crude gas passes to a mixing chamber, where it is quenched with cool, scrubbed, recycle gas. This quenching lowers the bulk temperature below the softening point of the entrained ash; part of the solidified ash may drop out at this point. The gas passes to waste heat boilers to generate superheated steam at 1500 psig, 900°F. After further indirect cooling, it is scrubbed with a large quantity of process condensate to remove the last traces of entrained particles. Some of the sulfur compounds are also removed in scrubbing (not shown in Table 18).

Water-Gas Shift Reaction

The raw gas has an H_2/CO mol ratio of about 0.75:1* The shift reactors increase this ratio by the water-gas shift reaction. For a 1000-ton/day hydrogen plant fed with coal, it is required to shift 25420 lb-mol/h of CO to hydrogen in order to change the composition from 34.8 mol% hydrogen, 47.2 mol% CO, 18.0 mol% CO_2 to 55.6 mol% hydrogen, 0.3 mol% CO, 44.1 mol% CO_2.

*Hydrogen plants that use a coal feed produce a low H_2/CO ratio, so more shift is needed than for plants that use a feed of natural gas or vacuum residuum. Also, syngas plants do not require as much shifting, because a H_2/CO ratio of 2 or 3 is optimum for this use.

Details of this portion of the process are described separately for the two cases: Case 1, Conventional Heterogeneous Catalyst, and Case 2, Proposed Homogeneous Catalyst. The WGSR processes are sketched in Figure 11.

CONVENTIONAL HETEROGENEOUS CATALYST

Conventional heterogeneous WGSR catalysts are preceded by a sulfur removed step (not shown) to protect the LT catalyst. The H_2S and about 80% of the COS are removed.

$$COS + H_2O \longrightarrow CO_2 + H_2S \qquad (55)$$

Three parallel lines are used for the heterogeneous shift reaction. Each line contains six parallel packed reactors. The top section of each reactor is packed with 1997 ft^3 of pellets of a Co/Mo high-temperature shift catalyst, such as Girdler's C-12-305, priced at \$135/ft^3.

Water is injected for cooling, and the gas then passes downward over 1511 ft^3 of pellets of a Cu/Zn sulfur-intolerant low-temperature shift catalyst in the bottom of each of the 18 reactors. Girdler's C18/8/C is a suitable catalyst (\$190/ft^3).

PROPOSED HOMOGENEOUS CATALYST

Preliminary sulfur removed is not required. Sulfur is removed later, during acid gas scrubbing.

Three parallel lines are used for the shift reaction. The total amount of shift catalyst required is 254.2 lb mols, ***provided that*** the catalyst system exhibits a turnover of 100 (mols CO converted per mol catalyst per hour). This turnover exceeds that demonstrated to date in laboratory experiments; it represents a goal to be attained if the economics presented in this evaluation are to be realized. Eighteen reactors are used in three parallel trains to contain a total of 165,000 gal of 10 wt% solution. Reactor configuration has not been worked out in detail.

The catalyst solution is pumped through an external cooler associated with each reactor to remove the exothermic heat of reaction and maintain reactor temperature of the desired level.

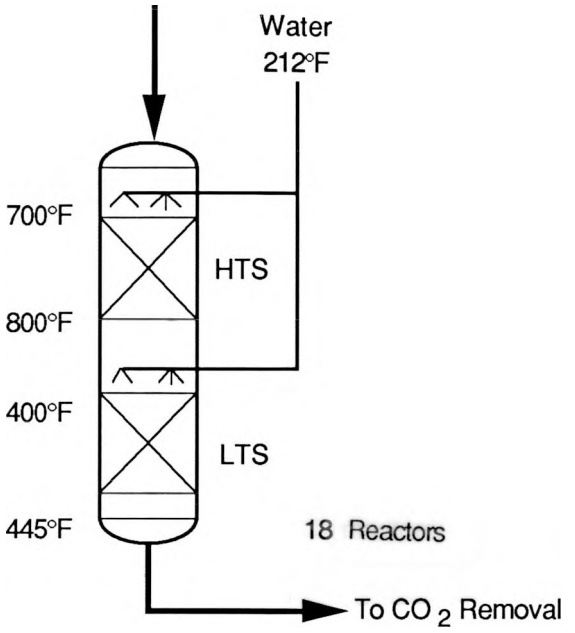

(**a**) Conventional heterogeneous water gas shift reaction.

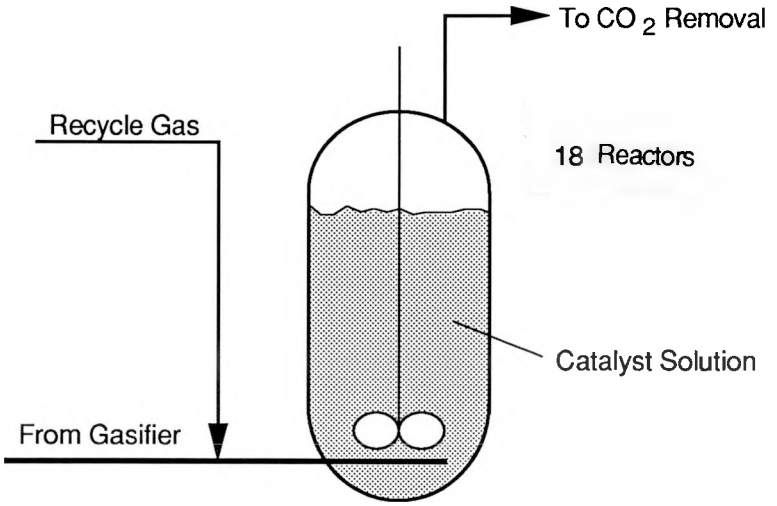

(**b**) Proposed homogeneous water gas shift reaction.

RA-M-1264-13

Figure 11. WGS reactor diagrams.

Acid Gas Removal

Three parallel lines are used for acid gas removal. The cooled gas stream (stream 9 in Figure 10) is processed in a Rectisol® unit for acid gas removal. Refrigerated methanol is used to absorb sulfur compounds and carbon dioxide. Remaining traces of sulfur are removed from the hydrogen in a guard bed of zinc oxide, which is replaced every six months.

Operating conditions of the Rectisol® process are proprietary. The fat absorbent is depressured slightly to release hydrogen, which is compressed and returned to the absorber. Other absorbed gases are then stripped from the methanol in a three-step regeneration entailing pressure letdown, nitrogen stripping, and thermal stripping.

Depressuring produces a CO_2-rich off-gas stream that contains substantial amounts of CO and hydrogen and is used as fuel in the boiler plant (stream 12). The fat absorbent is then stripped with nitrogen to release the bulk of the CO_2. This stream (11), consisting primarily of CO_2 and nitrogen, can be discharged directly to the atmosphere. [CO_2 can be recovered for sale, but no provisions for this have been included in the process we are evaluating here.] Finally, the methanol is heated to release an H_2S-rich acid gas stream (stream 10) suitable for sulfur recovery in a Claus unit. The treated hydrogen product (stream 13) leaves the unit essentially free of sulfur compounds. The system is designed to leave only 0.3% of CO_2 in the product gas. (This CO_2 is removed by methanation: see below.)

Sulfur Recovery

A single line is used for sulfur recovery. The H_2S-rich stream from the Rectisol® unit is sent to a conventional two-stage Claus plant for converting H_2S to elemental sulfur. The process entails the combustion of one-third of the H_2S to SO_2, followed by reaction of this SO_2 with the remaining H_2S over an activated alumina catalyst to form elemental sulfur. The sulfur is produced as a liquid and then is flaked for shipment.

$$H_2S + 1.5O_2 \longrightarrow SO_2 + H_2O \qquad (56)$$

$$2\,H_2S + SO_2 \longrightarrow 2H_2O + 3S \qquad (57)$$

A Beavon process treating unit reduces the residual sulfur content of the Claus plant tail-gas stream to an environmentally acceptable level and produces additional elemental sulfur. First, all sulfur species are converted to H_2S by catalytic hydrogenation, then the H_2S is absorbed in a solution containing anthraquinone disulfonic acid and vanadium salts, and the H_2S is converted to sulfur in an air-blowing operation (Stretford process). Sulfur is separated from the solution as a froth, then filtered and melted to obtain a high purity product. Exhaust gas from the Beavon plant is discharged to the atmosphere. Overall sulfur recovery in the Claus tail-gas units exceeds 99.9%.

Methanation

Three parallel lines are used for methanation. Hydrogenation over a nickel oxide catalyst at 500-625°F, 935 psig produces methane and reduces the content of CO and CO_2 below 10 ppm (by volume) each:

$$CO + 3H_2 \longrightarrow CH_4 + H_2O \quad (58)$$

$$CO_2 + 4H_2 - \longrightarrow CH_4 + 2H_2O \quad (59)$$

For most hydrogen applications, trace amounts of methane are an acceptable impurity, but CO and CO_2 are undesirable.

CAPITAL COST INVESTMENT

Estimates of the capital costs for 1000 tons/day hydrogen plants by each of the two cases are given in Table 19.

Battery Limits Investment

The battery limits investment is separated into costs by section. For this preliminary evaluation, we assume that the capital costs of the two cases differ only in the WGSR section and in the catalyst reactivation section, which appears only in Case 2. (The catalyst in Case 1 is not reactivated, but is discarded after three years and replaced.) This is a great simplification. We have focused on the section where there are the greatest differences between the two cases, particularly in the reactors themselves. Reactor auxiliaries were not evaluated in detail.

Table 19

MANUFACTURE OF HYDROGEN FROM COAL

Capital Cost Estimate

Cost Index = 485

WSGR Catalyst:	Case 1 Heterogeneous	Case 2 Homogeneous
TOTAL CAPITAL, $1,000		
Coal Storage and Preparation	16,462	16,462
Air Separation and Oxygen Compression	171,270	171,270
Coal Grinding, Slurrying, Gasification and Ash Handling	168,031	168,031
Heat Recovery and Gas Scrubbing	2,692	2,692
Water Gas Shift Reaction	24,000	8,884
Catalyst Reactivation	0	3,500
Heat Recovery	3,196	3,196
Acid Gas Removal	149,799	149,799
Methanation	7,875	7,875
Sulfur Removal and Recovery	13,753	13,753
TOTAL BATTERY LIMITS	557,078	545,462
Steam and Power Generation	39,551	39,551
Other Utilities	32,147	32,147
Product Storage	27,052	27,052
Offsites	49,457	49,457
TOTAL UTILITIES AND OFFSITE FACILITIES	148,207	148,207
TOTAL FIXED CAPITAL	705,285	693,669
Catalyst Inventory	10,200	76,230
TOTAL FIXED CAPITAL+ Catalyst Inventory	715,485	769,899

We have assured that the acid gas removal costs are the same in both cases, although Case 1, which requires a preliminary sulfur removal step, will need more items of equipment.

In Case 1, the installed cost of the reactors and their auxiliaries is estimated at $24.0 million additional equipment required for upstream H_2S removal is not included. In Case 2, the installed cost of the smaller reactors and their auxiliaries is estimated at $8.9 million. A 1% purge of the circulating catalyst stream is withdrawn to catalyst treating facilities estimated to cost $3.5 million. The system is engineered to reduce the loss of valuable catalyst components to negligible levels, based on commercial experience with homogeneous rhodium catalysts such as those that are used in Union Carbide's process for making butyraldehyde from propylene.

Case 2 appears to have a small advantage in a lower fixed capital cost, $694 million versus $705 million, but the difference is within the accuracy of the estimates. The working capital is much higher in Case 2, due to the high investment in ruthenium-based catalyst ($76 million versus. $10 million). To gain a payout on this larger total investment, the operating costs for Case 2 must be lower.

Utilities Investment

In addition to the steam and power generation units, the utilities section includes facilities for raw water storage and filtration, boiler feedwater preparation, a recirculating cooling water system, including cooling towers, utility water and potable water system, fire water, plant air, instrument air, and inert gas, flare system, storm water collection, oily water treatment, and sanitary waste treatment. Differences in utilities investments between Case 1 and Case 2 are assumed to be minor. This is a deliberate simplification, because there will be some differences in the WGSR sections.

Offsites Investment

Offsite facilities include such necessary auxiliaries as the electrical system, interconnecting piping, site preparation, perimeter fencing, roads and parking areas, maintenance equipment, laboratory equipment, mobile equipment, fire protection equipment, buildings and furnishings, communications system, and railroads. Again differences in offsites investments between Case 1 and Case 2 are assumed to be minor.

PRODUCTION COSTS

Production costs for Cases 1 and 2 are summarized in Tables 20, 21, and 22. The only significant differences between the two cases are in the costs of catalyst per ton of hydrogen produced. In Case 1, the two shift catalysts are replaced every three years. The high-temperature shift catalyst has no salvage value, and the low-temperature shift catalyst has a 5% salvage value (based on its copper content). The cost of these catalysts is spread out over three years production of hydrogen for an average charge of ¢10.99/kg of hydrogen. Other catalysts in the plant add about 1¢/kg hydrogen.

In Case 2, the homogeneous WGSR catalyst is continuously renewed, so the net WGSR catalyst consumption is negligible. We assume that recovery of ruthenium is essentially quantitative. Long-term catalyst stability needs to be demonstrated. Other catalysts in the plant add about 1¢/kg hydrogen.

No credit is given for by-product nitrogen in either case, because we assumed that it is unlikely that an offtake for such a large amount of nitrogen could be developed.

The production cost for Case 2 is estimated at $1019 per metric ton of hydrogen, which is $121/ton lower than the cost of $1140 estimated for Case 1. The saving is attributed entirely to the lower consumption of catalyst and would be smaller if experience showed catalyst losses were significant. When a return on invested capital is included, the product value of the hydrogen from Case 2 is $1661/metric ton, which is $75/ton below the product value of $1736 from Case 1. The Case 2 advantage is reduced because of the large inventory of costly ruthenium catalyst used in Case 2, however the Case 1 product value may be higher if significant costs are associated with upstream sulfur removal.

CONCLUSIONS

At the assumed WGSR turnover of 100, the product value of hydrogen made by a homogeneous WGSR catalyst is competitive with hydrogen produced in a conventional process with a heterogeneous WGSR catalyst. As a rough estimate, a turnover of about 50 is required for a breakeven operation. A substantial advantage to homogeneous WGSR could warrant a change and justify the substantial costs of development.

Table 20

MANUFACTURE OF HYDROGEN FROM COAL

Case 1- Conventional Heterogeneous WGSR Catalyst

PRODUCTION COST SUMMARY

RAW MATERIAL AND UTILITY COST

U.S.PEPCOST INDEX=485

LOCATION : U.S.GULF COAST

RAW MATERIALS	Unit Cost	Consumption /mt H2	¢/kg H2
Bituminous Coal at Mine	2.40 ¢/kg	7.372 mt	17.69
Coal Transport	3.31 ¢/kg	7.372 mt	24.40
Ash Disposal	0.55 ¢/kg	0.85 mt	0.47
Catalysts and Chemicals			11.99
Gross Raw Material Cost			54.55
UTILITIES			
Cooling Water	1.4 ¢/m3	220 m3	0.31
Steam	9.15 $/mt	3 mt	2.75
Process Water	17.7 ¢/m3	0.79 m3	0.01
Electricity	3.4 ¢/kWh	81.5 kWh	0.28
TOTAL			3.34
BY-PRODUCT CREDIT			
Sulfur	10.54 ¢/kg	0.255 mt	2.69
Nitrogen	0 ¢/kg	25.625 mt	0.00
TOTAL			2.69

Table 21

MANUFACTURE OF HYDROGEN FROM COAL

Case 2- Proposed Homogeneous WGSR Catalyst

PRODUCTION COST SUMMARY

RAW MATERIAL AND UTILITY COST

U.S.PEPCOST INDEX=485

LOCATION : U.S.GULF COAST

RAW MATERIALS	Unit Cost	Consumption /mt H2	¢/kg H2
Bituminous Coal at Mine	2.40 ¢/kg	7.372 mt	17.69
Coal Transport	3.31 ¢/kg	7.372 mt	24.40
Ash Disposal	0.55 ¢/kg	0.85 mt	0.47
Catalysts and Chemicals			1.00
Gross Raw Material Cost			43.56
UTILITIES			
Cooling Water	1.4 ¢/m3	220 m3	0.31
Steam	9.15 $/mt	3.1 mt	2.84
Process Water	17.7 ¢/m3	0.79 m3	0.01
Electricity	3.4 ¢/kWh	81.5 kWh	0.28
TOTAL			3.44
BY-PRODUCT CREDIT			
Sulfur	10.54 ¢/kg	0.255 mt	2.69
Nitrogen	0 ¢/kg	25.625 mt	0.00
TOTAL			2.69

Table 22

MANUFACTURE OF HYDROGEN FROM COAL

Comparisc n of Heterogeneous and Homogeneous Catalysts

INVESTMENT AND PRODUCTION COST

		Case 1	Case 2
Plant Size, thousands of metric tons/y PB		300	300
WGSR Catalyst		Heterogeneous (conventional)	Homogeneous (proposed)
INVESTMENT, US $ MILLION			
Battery Limits		557.1	545.5
Fixed Capital		705.3	693.7
Catalyst Inventory		10.2	76.2
PRODUCTION COSTS, US¢/KG H2			
Raw Materials (less by-product credit)		51.86	40.87
Utilities		3.34	3.44
Variable Costs		55.21	44.31
Maintenance Materials	3 % of battery limits	5.57	5.46
Operating Supplies		0.27	0.27
Operating Labor	41 /shift @$22.69/hr	2.72	2.72
Maintenance Labor	3 % of battery limits	5.57	5.46
Control Laboratory		0.54	0.54
Total Direct Costs		69.88	58.75
Plant Overhead		7.06	6.97
Taxes and Insurance	2 % of fixed capital	4.70	4.62
Depreciation	10 % of fixed capital	23.51	23.12
Plant Gate Cost		105.16	93.47
G&A, Sales, R&D	5 % of product value	8.81	8.44
Production Cost			
at 100% capacity		113.97	101.91
at 75% capacity		134.01	121.57
at 50% capacity		174.07	160.88
Product Value [Production Cost + 25%/yr return on (fixed capital + catalyst inventory)]			
at 100% capacity		173.60	166.07
at 75% capacity		213.51	207.11
at 50% capacity		293.32	289.20

Some other variations were explored briefly as summarized in Table 23.

Table 23. OTHER VARIATIONS IN HYDROGEN PRODUCTION

WGSR Catalyst	Cost ($/tr.oz)	Turnover, (hr^{-1})	Catalyst Inventory ($MM)	H_2 Product Value ($/mt)
Ru	70	100	76.2	1661
Ru	35	100	38.1	1627
Ru	70	80	95.3	1680
Ru	70	50	152.5	1741
Mo	1	100	1.1	1595
Mo	1	10	10.9	1715
Mo	1	5	21.8	1854
Heterogeneous (Case 1) (for comparison)				1736

A less costly WGSR catalyst might be an attractive competitor for hydrogen production from coal. A molybdenum catalyst has been suggested to replace ruthenium. Molybdenum is not as active as ruthenium, but its lower cost would permit breakeven operation at a lower turnover number. We have made some approximate calculations for a Mo-based homogeneous WGSR catalyst, taking into account the higher reactor volume required at lower turnover. Using some very broad assumptions, we tentatively conclude that a breakeven operation could be obtained at a turnover just below 10. However, these preliminary estimates are based on a WGSR catalyst solution that contains 10% by weight of the catalyst metal. For the case of Mo, this is a higher value than has been demonstrated in the laboratory to be effective. In the laboratory, a leveling off of catalyst activity was observed for Mo solutions that were still very dilute. Such dilute solutions would require much higher activity for breakeven operation.

CONCLUSIONS AND RECOMMENDATIONS

Conclusions

From our survey of the literature, we selected 10 catalysts for screening as potential catalysts for a homogeneously catalyzed WGS process. These catalysts were screened for activity and sulfur tolerance in batch reactors using simulated oxygen blown coal gas and low vapor pressure solvents. Several of these catalysts exhibited good sulfur tolerance, and two of them were chosen for further evaluation (ruthenium carbonyl with amine base in etheral solvents and molybdenum carbonyl with alkali base in alcoholic solvents). These catalysts were evaluated briefly in a continuous-flow reactor and the results were used as a basis for a preliminary economic analysis.

The economic calculations show that breakeven operation for hydrogen produced by homogeneous catalysis of the WGS reaction (hydrogen product value would be approximately equivalent with that from state-of-the art heterogeneous catalysis of the WGS) would occur with the ruthenium catalyst at TF = 50 and for the molybdenum catalyst at TF < 10. We have observed values as high as 86 for ruthenium catalysts and greater than 250 for the molybdenum catalyst. Values much greater have been observed for ruthenium catalysts in the literature (as high as 574[52]); however, our observation of TF = 250 is the highest value ever observed for molybdenum (to our knowledge), and most reported values have been in the range of TF < 10. Thus it would appear that homogeneous catalysis of WGS might offer significant advantages over the state-of-the-art heterogeneous process. The best case from continuous-flow reactor studies would appear to offer a cost advantage of $140 per metric ton (Mo catalyst with T F = 92). However, several assumptions had to be made to make these economic calculations, and a few of them are worth evaluating in more detail here.

Let's define a new figure of merit called volumetric rate (VR) defined as moles of product per liter of solution per hour.

$$VR\left(\frac{\text{moles } H_2}{\text{liter}\cdot\text{hr}}\right) = TF\left(\frac{\text{moles } H_2}{\text{moles Cat}\cdot\text{hr}}\right)\cdot C\left(\frac{\text{moles catalyst}}{\text{liter}}\right) \qquad (60)$$

Thus this figure of merit will be somewhat similar to the space-time-yield (STY) that is sometimes used by chemical engineers, except that the volume used here will be volume of solution rather than reactor volume and this is a rate rather than a yield value. The volumetric rate (VR) is the figure of merit for homogeneously catalyzed processes.

For the base case considered in the economic calculations, the volumetric rate was defined as 18.5 (25,420 lb-mol of H_2 in 165,000 gallons). The highest volumetric rate considered was VR = 33 moles of product/liter of solution/h (assuming 10 wt% ruthenium solutions, solution density of 1, and TF = 100). The breakeven case was half the base case at VR = 9. The breakeven case for molybdenum has a VR = 10 (assuming 10 wt% molybdenum, solution density of 1, and TF < 10). These VR values are high compared with commercial operations producing commodity chemicals by homogeneously catalyzed processes such as Union Carbide's rhodium-catalyzed production of n-butyraldehyde, which operates at VR = 0.74 (1.4×10^{-3} M Rh and 530 TF). Perhaps higher valued products can afford to operate at lower VR.

Experimentally in this project, the maximum VR observed for ruthenium was 0.58 (6.7×10^{-3} M, TF = 86, batch reactor). This value is intriguingly close to a commercially feasible value (that for the butyaldehyde process), but considerably below that assumed in the economic calculations. Although this is the maximum VR for Ru, most of our studies were conducted at VR around 0.19 (6.7×10^{-3} M Ru, TF = 28, batch reactor). No effort was made in this study to optimize VR for any system. For molybdenum, the maximum observed VR was 0.13 (5.4×10^{-2} M Mo, TF = 2.35, batch reactor) and did not vary much even if the turnover frequency varied considerably such that VR = 0.12 at the maximum TF of greater than 250 (4×10^{-4} M Mo, TF = 290, batch reactor). The maximum VR observed in the continuous-flow reactor was 0.15 (TF = 93 and 1.67×10^{-3} M Mo).

We have studied the sensitivity of the economic analysis to several factors related to the homogeneous catalyst (see Table 23). For example, lowering the catalyst cost by a factor of 2 (from 70 to 35) would have the effect of decreasing the product value by 2%, while lowering the catalyst cost by a factor of 70 (Ru at 70 versus Mo at 1) would decrease the product value by 4%. Increasing the turnover frequency by a factor 10 (Mo at TF = 10 versus Mo at TF = 100) decreases the product value by 7%. The sensitivity of the economic analysis to VR was not determined.

The other significant assumption in the economic analysis that needs to be discussed is the assumption that the precious metal can be completely recovered and

regenerated as Union Carbide is able to do in the butraldehyde process. Since the catalyst precursor is the ruthenium carbonyl, we anticipate that this assumption is a good one, but at this point we have no laboratory experience to justify the assumption. However, we have also not measured the catalyst activity over long periods of time and therefore do not have an indication of how often the regeneration must take place (what takeout ratio).

In summary, homogeneous catalysts do show activity for the WGSR under practical reaction conditions, at low temperature, and with good sulfur tolerance. The activities observed in this study are high enough to make homogeneous catalysis of the WGSR a potentially attractive option compared with present practiced technology.

Recommendations

The DOE must decide what level of cost savings would be necessary to continue the development effort. If the goal of this program was to make hydrogen from coal competitive with current hydrogen from natural gas sources, we are far from that level. Current prices of hydrogen from natural gas are running $735 per metric ton.[98] If however the goal of this effort is to have the best available technology ready for the day when it becomes necessary to produce hydrogen from coal or if the goal is to have the most economical production of hydrogen from coal for integrated advanced coal liquefaction plants, then the homogeneous route is worth pursuing.

The first recommendation is that the sensitivity of the economic analysis to volumetric rate (VR) be studied over a wide range of VR. It is possible that the homogeneous catalytic systems studied in this project are performing sufficiently to provide $100 to $150 per metric ton savings over the heterogeneous case if the economics are not very sensitive to VR. In addition, the cost of sulfur removal upstream of the heterogeneous WGS reactor has not been considered and therefore the cost savings of the homogeneous case could be considerably greater if this is a significant cost.

The lifetime of the catalyst is an important issue that has not been addressed experimentally and must be addressed for further development. For the economic analysis, we have assumed that 1% of the solution is constantly purged to send to the catalyst regenerator. If these catalysts are more robust than those used in the Union Carbide butyraldehyde process, then less solution would have to be routed to the regenerator which would result in a downsizing of the regenerator and lowering of the capital investment.

Finally, several specific catalyst issues that were not addressed need to be addressed:

(1) No attempt has been made, to date, to develop homogeneous WGS catalysts with high solubility in high boiling solvents appropriate for continuous operation. Regardless of the sensitivity of the economics to the volumetric rate (VR), it will always be desirable to have catalysts with improved solubility and high activity. Catalysts with higher solubilities can be designed by derivatizing the stabilizing ligands. One example of such an approach was screened in this project (system 10, meta-monosulfonated triphenylphosphine rhodium). This particular ligand was designed to impart high aqueous solubility to the catalyst and was reported to have high activity.[82] The results in our screening test were disappointing, possibly because Rh is sensitive to sulfur poisoning, but this approach should be pursued. Higher solubility with high activity, is particularly desirable for the Mo based catalysts.

(2) A thorough study of the effect of temperature on activity in a continuous-flow reactor is recommended. The very high activities reported in the literature were measured at 100°C.[52] Haenel et al. reported significantly higher activities by raising the temperature above 250°C.[93] We recommend that a thorough study of activity in the range 100 to 250°C be conducted for some of the more promising catalysts.

(3) Other highly active catalysts reported in the literature since we began this project appear worth pursuing in more detail, particularly the $K[Ru^{2+}(Hedta)(CO)]$ catalyst reported by Khan.et al. They reported TF = 350 at 50°C and 1 atm CO. This catalyst should be subjected to the same vigorous tests that we performed in evaluation of the catalysts discussed in this report. Also the mixed-metal cobalt rhodium catalyst ($Co_2Rh_2(CO)_{12}$) studied by Venäläinen et al.[67] should be tested for sulfur tolerance.

(4) The ruthenium/amine catalyst system suffers from disproportionation of the amine which may limit its usefulness in continuous operation. The development of amine cocatalysts that donot suffer this problem is highly desirable.

REFERENCES

1. a. C. L. Thomas, Catalytic Processes and Proven Catalysts (Academic Press, New York, 1970).

   b. M. I. Temkin, *Adv. Catal.* **1979**, *28*, 263-267.

   c. Catalyst Handbook (Springer-Verlag, London, 1970), Chapters 5 and 6.

2. R. M. Laine and R. B. Wilson Jr., Aspects of Homogeneous Catalysis, **1984**, *5*, 217.

3. R. M. Laine and E. J. Crawford, *J. Mol. Cat.* **1985**, *44*, 357.

4. J. W. Reppe, *Liebigs Ann. Chem.* **1953**, *582*, 1.

5. D. M. Fenton, U.S. Patent 3,490,872, 1970.

6. D. M. Fenton, U.S. Patent 3,539,298, 1970.

7. D. M. Fenton, U.S. Patent 3,781,364, 1973.

8. R. M. Laine, R. G. Rinker, and P. C. Ford, *J. Am. Chem. Soc.* **1977**, *99*, 252.

9. H. C. Kang, C. H. Mauldon, T. Cole, W. Slegeir, K. Cann, and R. Pettit, *J. Am. Chem. Soc.* **1977**, *99*, 8323-8325.

10. C. H. Cheng, D. E. Hendriksen, and R. Eisenberg, *J. Am. Chem Soc.* **1977**, *99*, 2791-2792.

11. V. N. Zudin, V. A. Likholobov, Yu. I. Yermakov, and N. K. Yeremenko, *Kinet. I Katal.* **1977**, *18*, 524.

12. P. C. Ford, *Acc. Chem. Res.* **1981**, *14*, 31-37.

13. D. C. Gross and P. C. Ford, *J. Am. Chem. Soc.* **1985**, *107*, 585-593.

14. E. L. Muetterties, *Inorg. Chem.* **1965**, *4*, 1841.

15. D. J. Darensbourg and J. A. Froelich, *J. Am. Chem.* **1977**, *99*, 4727-4729.

16. R. L. Kump and L. J. Todd, *Inorg. Chem.* **1981**, *20*, 3715-3718.

17. A. J. Deeming and B. L. Shaw, *J. Chem. Soc., A,* ***1969***, 443.

18. D. J. Darensbourg, *Isr. J. Chem.* **1977**, *15*, 247-252.

19. D. J. Darensbourg and A. Rokicki, *Organomet.* **1982**, *1*, 1685-1693.

20. K. R. Lane, R. E. Lee, L. Sallans, and R. R. Squires, *J. Am. Chem. Soc.*, **1984**, *106*,5767-5772.

21. N. Grice, S. C. Kao,and R. Pettit, *J. Am. Chem. Soc.*, **1979**, *101*, 1627-1628.

22. D. H. Gibson and T.-S. Ong, *Organomet.*, **1984**, *3*,1911-1913.

23. M. Catellani and J. Halpern, *I. Org. Chem.* **1980**, *3*,566-568.

24. T. Yoshida, Y. Ueda, and S. Otsuka, *J. Am. Chem. Soc.* ***1978***, *100*, 3941-3942.

25. J. R. Sweet and W.A.G. Graham, *Organomet.* ***1982***, *1*, 982-986.

26. R. A. Grey, G. P. Pez, and A. Wallo, *J. Am. Chem. Soc.*, 1**981**, *103*, 7536-7542.

27. D. J. Darensbourg, C. S. Day, and M. B. Fischer, *Inorg. Chem.* **1981**, *20*, 3577-3579.

28. D. J. Darensbourg, A. Rokicki, and M. Darensbourg, *J. Am. Chem. Soc.* **1981**, *103*, 3223.

29. R. Eisenberg and D. E. Hendriksen, *Adv. Catal.* **1979**, *28*, 79.

30. S. H. Strauss, K. H. Whitmire, and D. F. Shriver, *J. Organomet. Chem.* **1979**, *174*, C59-C62.

31. D. M. Vanderberg, T. M. Suzuki, and P. C. Ford, *J. Organomet. Chem.* **1984**, *272*, 309-320.

32. R. S. Paonessa and W. C. Trogler, *J. Am. Chem. Soc.* **1982**, *104*, 3529-3530.

33. a. T. Yoshida, T. Matsuda, and S. Otsuka, *ACS Symp. Ser.* **1981**, *152*, 79-94.
    b. T. Yoshida, T. Okano, Y. Ueda, and S. Otsuka, *J. Am. Chem. Soc.* **1981**, *103*,3411-3422.

34. a. R. G. Pearson and H. Mauermann, and*J. Am. Chem. Soc.* **1982**, *104*, 500-504.
    b. R. G. Pearson, H. W. Walker, H. Mauermann, P. C. Ford, *Inorg. Chem.* **1981**, *20*, 2741-2743.

35. J. A. Osborne, F. H. Jardine, J. F. Young, and G. Wilkinson, *J. Chem. Soc., A* **1966**, 1711-1732.

36. P. B. Chock and J. Halpern, *J. Am. Chem. Soc.* **1966**, *88*, 3511-3514.

37. E. L. Muetterties and P. L. Watson, *J. Am. Chem. Soc.* **1978**, *100*, 6978-6979.

38. L. Marko and F. Ungvary, *J. Organomet. Chem.* **1969**, *20*, 205.

39. J. R. Norton, *Acc. Chem. Res.* **1979**, *12*, 139.

40. J. P. Collman, R. G. Finke, P. L. Matlock, R. Wahren, R. G. Komato, and J. I. Brauman, *J. Am. Chem. Soc.* **1982**, *100*, 1119-1140.

41. J. C. Bricker, C. C. Nagel, and S. G. Schore, *J. Am. Chem. Soc.* **1982**, *104*, 1444-1445.

42. a. J. P. Collman and L. S. Hegedus, Principles of Organotransition Metal Chemistry,(Univ. Sci. Bks., Mill Valley, CA 1980), pp. 69-70.

    b. F. Cariati, R. Ugo, and F. Bonati, *Inorg. Chem.* **1966**, *5*, 1128-1132.

43. J. C. Bricker, C. C. Nagel, A. A. Bhattacharyya, and S. G. Shore, *J. Am. Chem. Soc.* **1985**, *107*, 377-384.

44. G. Blyholder, K-M. Zhao, and M. Lawless, *Organomet.* **1985**, *4*, 2170-2173.

45. T. Yoshia, T. Matsuda, T. Okano, T. Kitani, and S. Otsuka, *J. Am. Chem. Soc.* **1979**, *101*, 2027-2038.

46. T. Yoshida, T. Okano, K. Saito, and S. Otsuka, *Inorg. Chim. Acta.* **1980**, *44*, L135-L136.

47. M. G. Mason and J. A. Ibers, *J. Am. Chem. Soc.* **1982**, *104*, 5135-5157.

48. H. C. Kang, C. H. Mauldon, T. Cole, W. Slegeir, K. Cann, and R. Pettit, *J. Am. Chem. Soc.* **1977**, *99*, 8323-8325.

49. R. B. King, C. C. Frazier, R. M. Haines, and A. D. King, *J. Am. Chem. Soc.* **1978**, *100*, 2925-2927.

50. A. D. King, R. B. King, and D. B. Yang, *J. Am. Chem. Soc.* 1980, *102*, 1028-1032.

51. D. C. Gross and P. C. Ford, unpublished work.

52. W.A.R. Slegeir, R. S. Sapienza, and B. Easterling, *ACS Symp. Ser.* **1981**, *152*, 325-344.

53. R. B. Wilson and R. M. Laine, *J. Am. Chem. Soc.* **1985**, *107*, 361-368 and references therein.

54. Y. Shvo, Y. Rahamim, and D. Czerki, Paper 0 339, presented at the 13th International Conference on Organometallic Chemistry, Vienna, September 1985.

55. Y. Doi and S. Tamura, *Inorg. Chim. Acta.* **1981**, *54*, L235-L236.

56. C. C. Frazier, R. Hanes, A. D. King, Jr., and R. B. King, *Adv. Chem. Ser.* **1979**, *173*, 94-105.

57. W.A.R. Slegeir, R. S. Sapienza, R. Rayford, and L. Lam, *Organometallics*, **1982** *1*, 1728-1729.

58. B. H. Weiller, J-P. Liu, and E. R. Grant, *J. Am. Chem. Soc.* **1985**, *107*, 1595-1604.

59. R. J. Klingler, I. Bloom, and J. W. Rathke, *Organomet.* **1985**, *4*, 1893-1894.

60. R. M. Laine, *J. Am. Chem. Soc.* **1978**, *100*, 6451.

61. W. J. Thomson and R. M. Laine, *ACS Symp. Ser.* **1980**, *152*, 133-146.

62. P. Chini, G. Longoni, and V. Albano, *Adv. Organomet. Chem.* **1976,** *14*, 285 and references therein

63. K. Kaneda, M. Hiraki, K. Sano, T. Imanaka, and S. Teranishi, *J. Mol. Cat.* **1980**, *9*, 227-230.

64. a. P. C. Ford, R. G. Rinker, C. Ungermann, R. M. Laine, V. Landis, and S. A. Moya, *J. Am. Chem. Soc.* **1978**, *100*, 4595.
b. C. Ungermann, R. G. Rinker, P. C. Ford, V. Landis, S. A. Moya, and R. M. Laine, *Adv. Chem. Ser.* **1979**, *173*, 81.

65. R. M. Laine, *J. Org. Chem.* **1980**, *45*, 3370.

66. S.A.R. Knox, J. W. Koepke, M. A. Andrews and H. D. Kaesz, *J. Am. Chem. Soc.* **1975**, *97*, 3942.

67. T. Venäläunen, E. Iiskola, J. Pursiainen, T. A. Pakbanen, and T. T. Pakkanen, *S. Mol. Catalysis*, **1986**, *34*, 293.

68. R. Eisenberg,and C.-H. Cheng, U.S. Patent 4,107,076 (August 1978).

69. E. C. Baker, D. E. Hendriksen, and Eisenberg, *J. Am. Chem. Soc.* **1980**, *102*, 1020-1027.

70. T. C. Singleton, U.S. Patent 4,151,107 (April 1979).

71. D. Forster and T. C. Singleton, *J. Mol. Cat.* **1982,** *17*, 299-314.

72. P. A. Marnot, R. R. Ruppert, and J. P. Sauvage, *Nouv. J. Chim.* **1981**, *5*, 543-545.

73. J. P. Sauvage, P. Marnot, and R. Ruppert, French Patent No. 8,119-910.

74. E. Alessio, G. Clauti,and G. Mestroni, *J. Mol. Cat.* **1985**, *29*, 77-98.

75. H. Ishida, K. Tanaka, M. Morimoto, and T. Tanaka, *Organometallics* **1986**, *5*, 724.

76. D. Mahajan, C. Creutz, and N. Sutin, *Inorg. Chem.* **1985**, *24*, 2063-2067.

77. V. A. Likholobov, V. N. Zudin, and Yu I. Yermakov, *Proc. of The Fifth Jap.-Sov. Sem. Cat., Osaka, Japan*, **1980**, 9-18.

78. P. Gianoccaro, E. Pannacciulli, and G. Vasapollo, *Inorga. Chim. Acta.* **1985**, *96*, 179-185.

79. C. H. Cheng and R. Eiserberg, *J. Am. Chem. Soc.* **1978**, *102*, 5968-5970.

80. P. C. Ford, P. Yarrow, and H. Cohen, *ACS Symp. Ser.* **1981**, *152*, 95-106.

81. P. Yarrow, H. Cohen, C. Ungermann, D. Vandenberg, P. C. Ford, and R. G. Rinker, *J. Mol. Cat.* **1983**, *22*, 239-256.

82. J. Kaspar, R. Spogliarch, A. Cernogoraz, and M. Graziani, *J. Organomet. Chem.* **1983**, *255*, 371-376.

83. C. P. Kubiak and R. Eisenberg, *J. Am. Chem. Soc.* **1980**, *102*, 3627-3639,

84. C. P. Kubiak, C. Woodcock, and R. Eiserberg, *Inorga. Chem.* **1982**, *21*, 2119-2128.

85. B. R. Sutherland and M. Cowie, *Organomet.* **1985**, *107*, 1638-1648.

86. A. A. Frew, R. H. Hill, L. Manojovic-Muir, K. W. Muir, and R. J. Puddephatt, *J. Chem. Soc., Chem. Comm.* **1982**, 198-200.

87. J. R. Fisher, A. J. Mills, S. Sumner, M. P. Brown, M. A. Thomson, R. J. Puddephatt, A. A. Frew, L. Manojovic-Muir, and K. W. Muir, *Organomet. Chem.* **1982**, *1*, 1421-1429.

88. A. D. King, R. B. King, and D. B. Yang, *J.C.S. Chem. Comm.* **1980**, 529-530.

89. D. J. Darensbourg, A. Rokicki, and R. Kudaroski, *Organometallics* **1982**, *1*, 1161-1166 and references therein.

90. D. J. Darensbourg and C. Ovalles, *J. Am. Chem. Soc.* **1984**, *106*, 3750.

91. D. C. Elliot, L. J. Sealock Jr., and R. S. Butner, *Ind. Eng. Chem. Prod., Res. Dev.* **1986**, *25*, 541.

92. R. B. King, A. D. King Jr., and D. B. Yang, *ACS Symp Ser.* **1981**, *152*, 123.

93. M. W. Haenel, L. Schanne, and E. Wöstefeld, *Erdöl und Kohbe-Endgas-Petrochemie vereinigt mit Brennstoff-Chemie*, **1986**, *39*, 505.

94. D. J. Darensbourg and A. Rokicki, *ACS Symp. Ser.* **1981**, *152*, 107.

95. K. E. Lewis, D. M. Golden, and G. P. Smith, *J. Am. Chem. Soc.* **1984**, *106*, 3905.

96. M.M.T. Khan, S. B. Halligudi, and S. Shukla, *Angew. Chem. Int. Ed. Engl.* **1988**, *27*, 1735.

97. F. M. Gottschalk and G. J. Hutchings, *Appl. Catalysis* **1989**, *51*, 127

98. SRI PEP Yearbook International, 1989, SRI International, Menlo Park, CA.